
How explainable are adversarially-robust CNNs?

Mehdi Nourelahi [§]
mnourela@uwyo.edu

Lars Kotthoff [§]
larsko@uwyo.edu

Peijie Chen [†]
peijie.chen.auburn@gmail.com

Anh Nguyen [†]
anh.ng8@gmail.com

[§]University of Wyoming [†]Auburn University

Abstract

Three important criteria of existing convolutional neural networks (CNNs) are (1) test-set accuracy; (2) out-of-distribution accuracy; and (3) explainability. While these criteria have been studied independently, their relationship is unknown. For example, do CNNs that have a stronger out-of-distribution performance have also stronger explainability? Furthermore, most prior feature-importance studies only evaluate methods on 2-3 common vanilla ImageNet-trained CNNs, leaving it unknown how these methods generalize to CNNs of other architectures and training algorithms. Here, we perform the first, large-scale evaluation of the relations of the three criteria using 9 feature-importance methods and 12 ImageNet-trained CNNs that are of 3 training algorithms and 5 CNN architectures. We find several important insights and recommendations for ML practitioners. First, adversarially robust CNNs have a higher explainability score on gradient-based attribution methods (but not CAM-based or perturbation-based methods). Second, AdvProp models, despite being highly accurate more than both vanilla and robust models alone, are not superior in explainability. Third, among 9 feature attribution methods tested, GradCAM and RISE are consistently the best methods. Fourth, Insertion and Deletion are biased towards vanilla and robust models respectively, due to their strong correlation with the confidence score distributions of a CNN. Fifth, we did not find a single CNN to be the best in all three criteria, which interestingly suggests that CNNs are harder to interpret as they become more accurate.

1 Introduction

Feature importance [1, 5] is a well-known method for explaining a classifier’s decisions by an *attribution map* (Fig. 1), which highlights the input pixels that are important for or against a given label. Attribution maps (AMs), a.k.a. “saliency maps”, can be useful for many tasks including localizing malignant tumors in x-ray images [41], detecting objects in a scene [61], discovering biases in image classifiers [31], and explaining image similarity [23]. Most AM methods are *posthoc* explanation methods and can be conveniently applied to any convolutional networks (CNNs). Despite their wide applicability, state-of-the-art AM methods, e.g. [1, 48, 61], are often evaluated on the same set of ImageNet-trained vanilla classifiers (mostly AlexNet [30], ResNet-50 [24], or VGG networks [49]). Such limited evaluation raises important questions on how an AM method generalizes to other models that are trained differently or of different architectures.

In this paper, we analyze the practical trade-offs between three essential properties of CNNs: (1) test-set accuracy; (2) out-of-distribution (OOD) accuracy [3, 36]; and (3) explainability of their AMs [5]. That is, we perform the *first* large-scale, empirical, multi-dimensional evaluation of 9 state-of-the-art

AM methods, each on 12 different models for 5 different CNN architectures. That is, using 4 common evaluation metrics, we assess each AM method on 5 vanilla classifiers and 5 adversarially robust models, i.e. of the same architectures but trained via adversarial training [35, 56]—a leading training framework that substantially improves model accuracy on OOD data. Comparing vanilla and robust models is important because robust models tend to generalize better on some OOD benchmarks [9, 56, 57, 60] but at the cost of worse test-set accuracy [35, 58]. Interestingly, robust models admit much smoother (i.e., more interpretable) gradient images [5, 16, 60], which questions whether robust models are more *explainable*¹ than their vanilla counterparts when using state-of-the-art AM methods. Our key findings are:

1. Robust models are more explainable than vanilla ones under gradient-based AMs but not CAM-based or perturbation-based AMs (Sec. 3.1).
2. In contrast to vanilla and robust models, which are trained on either real and adversarial images, respectively [35, 58], CNNs trained on *both* real and adversarial data via AdvProp [56] are highly competitive on both test-set and OOD data. Yet, we find AdvProp models to be *not superior* in explainability compared to robust models (Sec. 3.2).
3. On all 12 models and under 4 different AM evaluation metrics, GradCAM [48] and RISE [39] are consistently among the top-3 best methods (Sec. 3.3). Thus, considering both time complexity and explainability, CAM and GradCAM are our top recommendations, which interestingly suggest that the field’s progress since 2017 may be stagnant.
4. We did not find *any CNNs* to be exactly the best in all three criteria: test-set accuracy, OOD accuracy, and explainability. For example, the models with the highest test-set accuracy, e.g. DenseNet, do not have the highest localization scores, suggesting that CNNs’ decisions are harder to interpret as they become more accurate in classification. Interestingly, we do find a competitive ResNet-50 CNN trained via AdvProp (PGD-1) to be all-around winner under three explainability metrics: Pointing Game, WSL, and Insertion (Sec. 3.4).
5. The Insertion [46] is heavily biased towards vanilla models while Deletion strongly favors robust models, which tend to output more conservative confidence scores. In general, these two score-based metrics strongly correlate with the mean confidence scores of classifiers and largely disagree (Secs. 3.5 & 3.6).

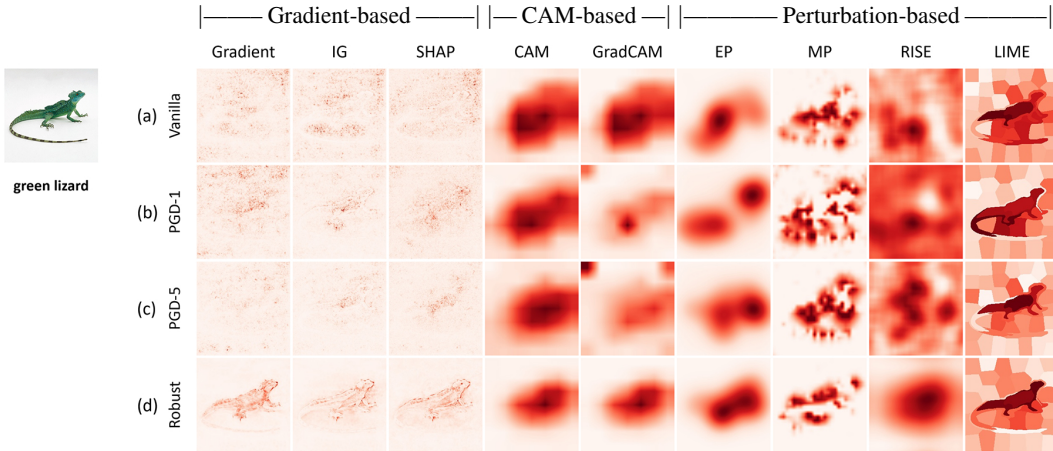


Figure 1: A comparison of attribution maps (AMs) generated by 9 AM methods for four different ResNet-50 models for the same input image and target label of “green lizard”. From top down: (a) vanilla ImageNet-trained ResNet-50 [24]; (b–c) the same architecture but trained using AdvProp [56] where adversarial images are generated using PGD-1 and PGD-5 (i.e. 1 or 5 PGD attack steps [35] for generating each adversarial image); and (d) a robust model trained exclusively on adversarial data via the PGD framework [35]. As CNNs are trained on more adversarial perturbations (from top down), the AMs by gradient-based methods tend to be less noisy and more interpretable. See Sec. A7 for more examples.

¹“explainable” here means scoring high on the four AM evaluation metrics in Sec. 2.4.

2 Methods and experimental setup

2.1 Datasets

To align with prior work [5, 17, 18, 61], we use the 50K-image ILSVRC 2012 validation set [45] to evaluate AM methods. First, to filter out ambiguous multi-object ImageNet images [7], we remove images that have more than one bounding box. Furthermore, to more accurately appreciate the quality of the heatmaps, we remove the images whose bounding box covers more than 50% of the image area because such large objects do not serve as a good measure to distinguish AM methods (on ImageNet, a simple Gaussian baseline already obtains $\sim 52\%$ weakly-supervised localization accuracy [10]). For the remaining images, like [5], we evaluate AMs on two ImageNet subsets: (a) we choose 2,000 random validation-set images; (b) for each architecture, we choose 2,000 images that a pair of (vanilla, robust) models correctly label (hereafter, ImageNet-CL) to understand the explainability of models in general vs. when they make correct predictions.

Table 1: Top-1 accuracy (%) of pre-trained networks and their confidence scores on ImageNet-CL.

Model name	Architecture	Training	Confidence	ImageNet acc.	Adv acc.
AlexNet	AlexNet [30]	vanilla	0.79 ± 0.21	56.55	0.18
AlexNet-R	AlexNet [30]	PGD [35]	0.41 ± 0.29	39.83	22.27
GoogLeNet	GoogLeNet [54]	vanilla	0.78 ± 0.22	69.78	0.08
GoogLeNet-R	GoogLeNet [54]	PGD [35]	0.49 ± 0.29	50.94	31.23
ResNet	ResNet-50 [24]	vanilla	0.89 ± 0.16	76.15	0.35
ResNet-R	ResNet-50 [24]	PGD [35]	0.56 ± 0.30	56.25	36.11
PGD-5	ResNet-50 [24]	AdvProp [56]	0.90 ± 0.15	77.01	73.55
PGD-1	ResNet-50 [24]	AdvProp [56]	0.91 ± 0.14	77.31	69.02
DenseNet	DenseNet-161 [26]	vanilla	0.90 ± 0.18	77.14	0.51
DenseNet-R	DenseNet-161 [26]	PGD [35]	0.66 ± 0.34	66.12	41.76
MobileNet	MobileNet-v2 [47]	vanilla	0.87 ± 0.23	71.88	0.01
MobileNet-R	MobileNet-v2 [47]	PGD [35]	0.41 ± 0.26	50.40	29.65

2.2 Image classifiers

We run AM methods on a large set of five ImageNet-pretrained CNN classifiers of five different architectures: AlexNet [30], GoogLeNet [54], ResNet-50 [24], DenseNet-161 [26], and MobileNet-v2 [47]. To understand the relationship between adversarial accuracy and explainability, we compare the vanilla models with those trained via adversarial training [35]. For completeness, we also evaluate AM methods on ResNet-50 models trained on a mix of real and adversarial data via AdvProp [56]. The robust models tend to have $\sim 1.8\times$ lower confidence scores, lower ImageNet accuracy, but much higher adversarial accuracy² than vanilla models (Table 1). In contrast, AdvProp-trained models have similar ImageNet accuracy and confidence scores to vanilla models, but higher adversarial accuracy than robust models (Table 1; PGD-1 & PGD-5).

2.3 Attribution methods

2.3.1 Gradient-based methods

Gradient [50] uses the gradient image, which measures the sensitivity of the confidence score of a target label to changes in each pixel. **Integrated Gradients** (IG) [53] ameliorates the gradient saturation problem by linearly interpolating between the input image and a reference zero image and averaging the gradients over all the interpolation samples.

SHapley Additive exPlanations (SHAP) [33] approximates Shapley values of a prediction by assessing the effect of deleting a pixel under all possible combinations of the presence and absence of the other pixels. While SHAP is theoretically grounded on the classic Shapley values, it often requires a larger sample size than IG (200 vs. 50) and thus slower.

²Following [5, 9], our PGD attacks use 7 steps per image; L_2 norm $\epsilon = 3$, and a step size = 0.5.

2.3.2 CAM-based methods

CAM [61] produces a heatmap by taking a weighted average of the channels at the last convolutional layer of a CNN where the channel weights are the weights of the fully-connected layer that connects the global averaged pooling (GAP) value of each channel to the network classification outputs. While CAM is a faithful explanation of a CNN’s “attention”, it is only applicable to CNN architectures that have the GAP layer right before the last classification layer. **GradCAM** [48] approximates a channel’s weight in CAM by the mean gradient over the activations in that channel and is applicable to all CNNs including those without a GAP layer.

2.3.3 Perturbation-based methods

Meaningful Perturbation (MP) [18] finds the smallest real-valued, Gaussian-blurred mask such that when applied to the input image it minimizes the target confidence score. MP is sensitive to changes in hyperparameter values [5]. To ameliorate the sensitivity to hyperparameters, Fong et al. [17] propose to average over four MP-like heatmaps of varying controlled sizes of the high-attribution region. **Extremal Perturbation** (EP) [17] is less sensitive to hyperparameter values than MP but requires 4 separate optimization runs to generate one AM.

While MP and EP are only applicable to models that are differentiable, **LIME** [43] and **RISE** [39] are two popular AM methods that are applicable to black-box CNNs, where we only observe the predictions. LIME generates N masked images by zeroing out a random set of non-overlapping superpixels and takes the mean score over the masked samples where the target superpixel is *not* masked out as the attribution. Like CAM, RISE also takes a weighted average of all channels but the weighting coefficients are the scores of randomly masked versions of the input image.

2.4 Evaluation metrics

Pointing Game (PG) considers an AM correct if the highest-attribution pixel lies inside the human-annotated bounding box; that is, the main object in an ImageNet image must be used by CNNs to predict the ground-truth label. We use the PG implementation of TorchRay [19].

Weakly Supervised Localization (WSL) [6, 61] is a more fine-grained version of PG. WSL computes the Intersection over Union (IoU) of the human-annotated bounding box and bounding box generated from an AM via threshold-based discretization. We use the WSL evaluation framework by [11] and consider an AM correct if the $\text{IoU} > 0.5$.

The **Deletion** metric [22, 39, 46] (\downarrow lower is better) measures the Area under the Curve (AUC) of the target-class probability as we zero out the top- N highest-attribution pixels at each step in the input image. That is, a faithful AM is expected to have a lower AUC in Deletion. For the **Insertion** metric [22, 39, 46] (\uparrow higher is better) we start from a zero image and add top- N highest-attribution pixels at each step until recovering the original image and calculate the AUC of the probability curve. For both Deletion and Insertion, We use the implementation by [38] and $N = 448$ at each step.

2.5 Hyperparameter optimization

Perturbation-based methods have explicit numeric hyperparameters and can be highly sensitive to their values [5]. As we are the first to compare AM methods across many CNN architectures and models, we tune the hyperparameters for each pair of (AM method, CNN) using grid search. The tuned hyperparameter and optimized values are listed in Sec. A1.

Computation resources Since the AM methods can be run in parallel for image batches, we run our experiments on four GeForce GTX Titan X, a Tesla P100 and a K80 GPU.

3 Experimental results

3.1 Robust models provide better gradient-based AM explanations than vanilla models

Robust models often achieve better accuracy than vanilla CNNs on OOD images [2, 9, 35, 56]. In terms of interpretability, robust models admit smoother gradient images [5] and smoother activation maps, i.e. internally filtering out high-frequency input noise [9]. As these two important properties

may highly improve the quality of AMs, it is interesting to test whether AMs generated for robust models are more explainable than those for vanilla models.

Experiments For each of the 12 CNNs, we run the 9 AM methods on 2,000 ImageNet-CL images. That is, for each CNN, we generate $9 \times 2,000 = 18,000$ images (for MobileNet and AlexNet CNNs, we only run 8 methods as CAM is not applicable to these GAP-less architectures). For each AM, we compute the 4 evaluation metrics and compare the distributions of scores between vanilla and robust models (detailed scores per CNN are in Sec. A5).

Localization results For PG and WSL, we find *no significant differences* between vanilla and robust AMs (Fig. 2; a–b) except for the gradient-based AMs where robust CNNs significantly outperform vanilla models (Mann Whitney U-test; p -value < 0.003). CAM-based AMs of these two types of CNNs are visually similar for most images (see Fig. 1a and d). The perturbation-based AMs are less similar and neither type of model outperforms the other significantly (Fig. 1). For all three gradient-based methods, the robust models’ AMs often clearly highlight the main object (Fig. 1), which is consistent with a comparison of SmoothGrad AMs [60].

Score-based results For all methods, we find a significant difference between the AMs of robust and those of vanilla models (Mann Whitney U-test; p -value < 0.002). For Insertion, vanilla models outperform robust models but robust models outperform vanilla models for Deletion (Fig. 2).

The results for ImageNet are similar to ImageNet-CL (see Fig. A5). Robust models have higher OOD accuracy and higher explainability under gradient-based AMs, but not CAM-based or perturbation-based AMs.

Recommendation ML practitioners should use CAM-based methods for either vanilla or robust models as there is no difference in explainability and CAM-based methods have fewer hyperparameters and run faster than perturbation-based AM methods.

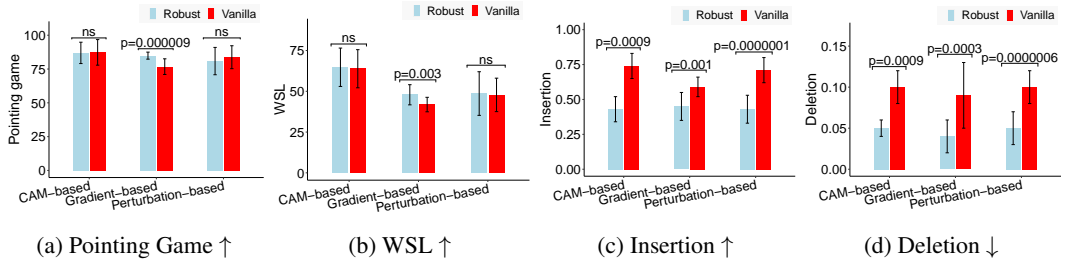


Figure 2: The AMs of robust models consistently score higher than those of vanilla models on Pointing Game [59] (a) and weakly-supervised localization (WSL) [61] (b). For Deletion (↓ lower is better), robust models consistently outperform vanilla models for all three groups of AM methods (d). In contrast, under Insertion, vanilla models always score better (c).

3.2 Training on both real and adversarial data improves classifiability but not explainability

Many high-stake applications, e.g. in healthcare, require CNNs to be both accurate and explainable [32]. AdvProp models, which are trained on both real and adversarial data, obtain high accuracy on both test-set and OOD data [56]—better than both vanilla and robust models in terms of classification accuracy. We test whether AdvProp CNNs offer higher explainability than vanilla and robust models.

Experiments We follow our setup above (Sec. 3.1) for four CNNs of the same ResNet-50 architecture: vanilla ResNet, PGD-1, PGD-5, and ResNet-R, and again compute all four metrics for ImageNet-CL.

Results The robust models have the best accuracy for object localization (Fig. 3; a–b) while vanilla models score the worst. Interestingly, AdvProp models are consistently performing in between vanilla and robust models; better than vanilla models under Insertion (Fig. 3c), and similar to vanilla models under Deletion (Fig. 3d).

The results for ImageNet are similar to those of ImageNet-CL (see Fig. A6).

Recommendation We recommend to always use AdvProp models instead of vanilla models since AdvProp models are not only more accurate in classification accuracy than vanilla models but also offer higher explainability under Pointing Game, WSL, and Insertion (Fig. 3a–c).

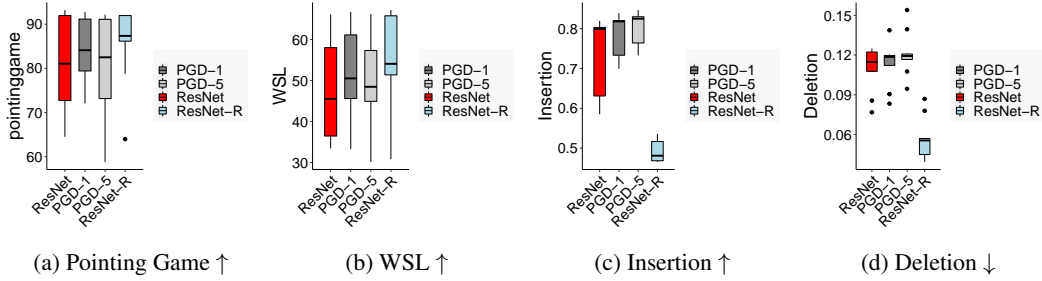


Figure 3: Averaging across 9 AM methods, AdvProp models (PGD-1 and PGD-5) outperform vanilla models (ResNet) but are worse than robust models (ResNet-R) in two object localization metrics (a & b). See Fig. 1 for qualitative results that support AdvProp localization ability. In Insertion, AdvProp models are also better than vanilla. We find the same conclusions for ImageNet images (Fig. A6).

3.3 GradCAM and RISE are the best feature attribution methods

Usually AM methods are only compared to a few others and only on vanilla ImageNet-trained CNNs [17, 18, 39, 53, 61]. It is therefore often unknown whether the same conclusions generalize to other non-standard CNNs that are trained differently or of novel architectures. Here, we aim to find out the best overall AM methods.

Experiments For each of the 8 AM methods (i.e. excluding CAM, which is not applicable to AlexNet and MobileNet), we average across the ten CNNs (Sec. 2.2) i.e. 5 vanilla and 5 robust CNNs, excluding two AdvProp models.

Results Fig. 4 shows that in terms of average ranking, as shown in Table A2, GradCAM and RISE are the best methods overall, closely followed by EP. Since the quantitative and qualitative results of CAM and GradCAM are almost identical (see Sec. A5 and Fig. 1), CAM would also be among the best AM methods, if applicable to a given CNN.

MP is the worst AM method on average. Besides the explainability, Table 2 shows the time complexity and runtime of the methods; GradCAM is the overall best.

In the literature, the simple Gradient [50] method often yields noisy saliency maps [5, 51, 53] on vanilla CNNs and is thus regarded as one of the worst AM methods. However, interestingly, when averaging its performance over all 10 CNNs (both vanilla and robust), the simple Gradient method outperforms the more complicated methods LIME, IG, SHAP, and MP in terms of both WSL (Fig. 4b) and runtime.

Again the results for ImageNet are similar to those on ImageNet-CL (see Fig. A8, Tables A2 & A3).

Recommendation Given an arbitrary CNN, we recommend using GradCAM or CAM.

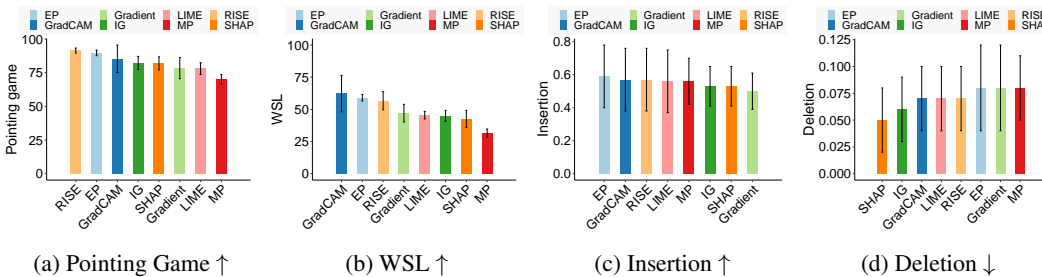


Figure 4: The average performance of 8 attribution methods across 10 CNNs show that GradCAM and RISE are among the top-3 for Pointing Game (a), WSL (b), Insertion (c), and Deletion (d) (↓ lower is better) while MP is the worst on average across all four metrics (see Table A2). The result of AM methods across four metrics on ImageNet is shown in Fig. A8.

Table 2: AM methods are ranked based on average WSL performance over 10 CNNs (excluding AdvProp models), runtime complexity, number of forward passes, number of backward passes, default hyperparameters, and median of runtime per image (in milliseconds).

Methods	WSL	# of Forward passes	# of Backward passes	$O(n)$	Hyperparameters	Runtime (ms)
CAM	67.63 ± 1.67	1	0	$O(1)$	n/a	108
GradCAM	62.29 ± 14.17	1	1	$O(1)$	n/a	34
EP	59.06 ± 2.53	$i (\# \text{ iterations}) \times a (\# \text{ areas})$	$i (\# \text{ iterations}) \times a (\# \text{ areas})$	$O(n)$	$N = 800, a = 4$	32,063
RISE	56.72 ± 7.03	$N (\# \text{ samples})$	0	$O(n)$	$N = 8,000$	8,485
Gradient	47.03 ± 6.88	1	1	$O(1)$	n/a	26
LIME	45.47 ± 2.91	$N (\# \text{ samples})$	0	$O(n)$	$N = 1,000$	7,234
IG	44.97 ± 4.23	$N (\# \text{ samples})$	$N (\# \text{ samples})$	$O(n)$	$N = 50$	196
SHAP	42.61 ± 6.63	$N (\# \text{ samples})$	$N (\# \text{ samples})$	$O(n)$	$N = 200$	1,137
MP	31.58 ± 3.12	$i (\# \text{ iterations})$	$i (\# \text{ iterations})$	$O(n)$	$N = 500$	7,530

3.4 CNN classification accuracy, explainability, and number of multiply-accumulate operations

It is a practical question, but under-explored in research, for ML practitioners: Which network to use given the classification accuracy vs. explainability criteria? Via our comprehensive experimental evaluation, here, for the first time, we investigate the best CNN overall.

Experiments From the experimental results described above, here, we analyze the ImageNet validation classification accuracy (see Table 1), explainability scores, and the number of multiply-accumulate operations (MACs) [24] (measured with [52]) of all 12 CNNs.

Results In WSL and Pointing Game, no CNN performs the best in both image classification and localization (Fig. 5a; the IDEAL region is empty). That is, higher accuracy is not correlated with better localization and there is a Pareto front with DenseNet-R, PGD-1, and ResNet-R. Interestingly, Insertion strongly correlates with the classification accuracy of CNNs (Fig. 5b) and the best CNNs under Insertion are DenseNet, PGD-1, and PGD-5.

While no CNN is the best among all four metrics, on ImageNet, we find PGD-1 CNN to perform the best among 12 CNNs under Pointing Game, WSL, and Insertion (see Fig. A9).

Recommendation ML practitioners should use AdvProp trained models to maximize the classification accuracy and explainability, here PGD-1 for the ResNet-50 architecture.

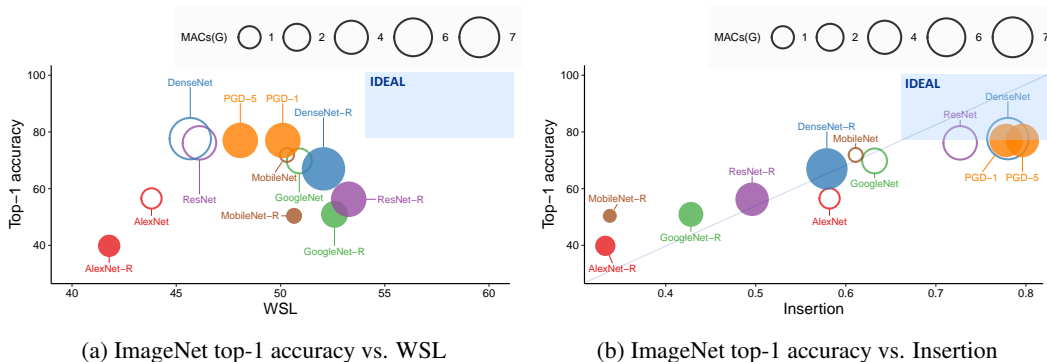
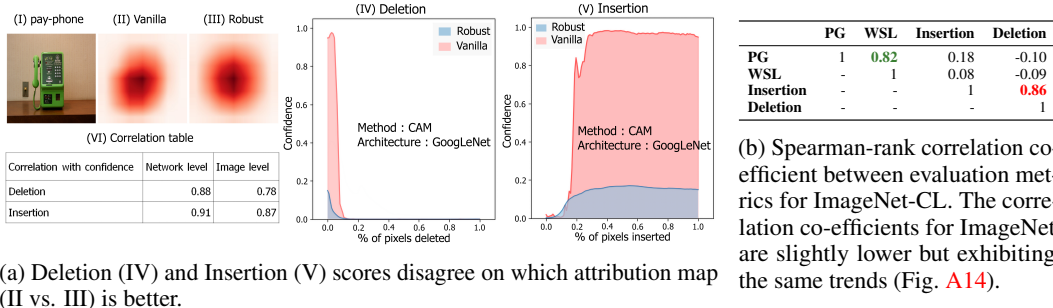


Figure 5: The average performance of all 12 CNNs across eight attribution methods under WSL and Insertion compared to ImageNet top-1 accuracy and MACs. No network is consistently the best across all metrics and criteria. Fig. A2 shows the results for the Pointing Game and Deletion metrics. The IDEAL region is where ideal CNNs of the highest classification and explanation capabilities are.

3.5 Insertion and Deletion are predictable from the confidence scores, regardless of the explanation quality

Insertion and Deletion are among the most common AM evaluation metrics in both computer vision [1, 15, 25, 39, 46, 55] and natural language processing [4, 12, 28, 40]. Yet, our results of comparing vanilla and robust models show some surprising phenomenon that all robust CNNs



(a) Deletion (IV) and Insertion (V) scores disagree on which attribution map (II vs. III) is better.

Figure 6: Insertion and Deletion scores are strongly correlated with a CNN’s confidence scores for an image regardless of heatmap quality (VI). For the same “pay phone” image (I), the CAM heatmaps of GoogleNet and GoogleNet-R are visually similar (II vs. III). Yet, under Deletion, the robust heatmap (III) is better. In contrast, under Insertion, the vanilla heatmap (II) is better. The **vanilla** AUC is always larger than the **robust** AUC (IV and V). That is, Insertion and Deletion are not exclusively measuring the quality of heatmaps, yielding misleading conclusions. More examples in Sec. A2.3.

consistently outperform vanilla CNNs on Deletion and the reverse is true under Insertion (Figs. 2 and 5). Therefore, we investigate whether this is because robust models tend to have much lower confidence than vanilla models (Table 1). That is, Insertion and Deletion scores might be simply reflecting the confidence score distribution of a CNN rather than the true explainability of the AMs.

Experiments We calculate the Spearman-rank correlation between confidence score and Deletion and Insertion score at both the network and image level. At the network level, we compute the Spearman-rank correlation coefficient between each CNN’s average confidence (over 2,000 ImageNet images) and their average Deletion (or Insertion) scores.

At the image level, we compute the Spearman-rank correlation between a single confidence score (given a CNN) and a Deletion score for each image. We repeat for all 10 CNNs and 9 AM methods.

Results We find a strong Spearman-rank correlation of 0.88 between CNN mean confidence score and mean Deletion score (Fig. 6a; VI table), and also a strong Spearman-rank correlation of 0.78 between an image’s confidence score and Deletion score (for all 10 CNNs, all 2,000 images and all AMs). The same conclusions are found at the image level (Fig. 6a; VI table). See Fig. 6a for qualitative results illustrating that the Deletion scores are mostly predictable from the confidence scores alone regardless of the actual heatmap quality.

Recommendation We do not recommend Insertion and Deletion for comparing the explainability of models that have dissimilar confidence-score distributions.

3.6 Insertion and Deletion can largely disagree and weakly correlate with localization metrics

Evaluating AMs is an open question [13, 14] and no automatic evaluation metric is yet a single best estimator of AM faithfulness. Therefore, the community resort to a suite of metrics (4 of them in this paper). Following upon the finding in Sec. 3.5 that Insertion and Deletion do not qualitatively reflect AM quality (but instead confidence scores), here, we quantify how the 4 metrics correlate with one another.

Experiments We compute a Spearman-rank correlation coefficient for each pair of metrics from all the AMs generated for ImageNet-CL images using all 12 CNNs and 9 methods.

Results First, we find that, when CNNs correctly classify images, Pointing Game and WSL strongly and positively correlate (Spearman-rank correlation of 0.82). However, these two localization metrics only weakly correlate with score-based metrics (Table. 6b; from -0.09 to 0.18). Importantly, Insertion and Deletion strongly disagree over all 12 CNNs tested (Table. 6b; 0.86). That is, a heatmap considered good under Insertion is highly likely to be considered bad under Deletion, and vice versa. We hypothesize that this divergence between Insertion and Deletion is due to the fact that our set of networks contain both vanilla and robust models, and that the two score-based metrics are reflecting the confidence-score distributions instead of the AM quality.

4 Related work

Generalization of attribution methods Most AM studies in the literature, e.g. [1, 5, 8, 17, 18, 48, 61], only tested AM methods on two or three of the following vanilla ImageNet-pretrained CNNs: AlexNet, ResNet-50, GoogLeNet, and VGG-16. Recent work found that AMs on robust models are less noisy and interestingly often highlight the outline of the main object. Yet, such comparisons [5, 9, 60] were done using only one AM method (vanilla Gradient in [5] or SmoothGrad in [60]). In contrast, our work is the first large-scale, systematic evaluation of 9 AM methods on an unprecedentedly-large set of 12 different ImageNet CNNs spanning 5 CNN architectures and 3 training algorithms (see Table 1). Over 12 CNNs, we find GradCAM to be the best-performing (among 9 tested AM methods) when considering all 4 metrics. This finding importantly suggests that the dozens of newer AM methods in the past 6 years are not better than GradCAM in general, maybe only for specific combinations of CNN and evaluation metrics.

Explainability of robust models Robust models were reported to have more interpretable *gradient* images [5, 35, 37, 44, 60] than those of vanilla CNNs. However, it is not yet known whether this superiority in interpretability remains when state-of-the-art AM methods are used. Our results of how 9 state-of-the-art AM methods perform on robust models provide important recommendations for the community when considering adversarial training or AdvProp in practice.

Score-based attribution evaluation metrics For assessing AMs, Deletion, Insertion, and other confidence-score-based metrics are widely used in both computer vision [1, 15, 25, 39, 46, 55] and natural language processing [4, 12, 28, 40]. However, deleting a pixel by zeroing it out is problematic. First, zeroing out a pixel can create OOD samples, which often cause CNNs to misbehave [1, 25]. Second, zeroing out a pixel can generate an image of different, unintended meanings to CNNs (e.g. zero pixels represent darkness in a matchstick image), potentially leading to evaluation scores inconsistent with human notions of interpretability [25, 27]. In contrast to prior work, we report a novel finding about score-based metrics: They are strongly correlated with the average probability scores of a CNN, rendering the comparison between vanilla and robust models under Deletion and Insertion extremely biased and conclusions misleading. To our knowledge, our finding is novel and different from a prior OOD-ness issue of Insertion and Deletion samples raised by Hooker et al. [25].

As in related work [20, 55], we find that Insertion and Deletion scores are highly correlated. However, our results find localization-based scores (WSL and PG) to *not strongly correlate* with these two score-based metrics and therefore measure a different characteristic of AMs.

5 Discussion and Conclusion

Limitations Our work is the first large-scale evaluation of many CNNs and many methods, which we cover three main sets of representative methods: gradient-based, perturbation-based, and CAM-based. Yet, there are naturally other methods not included in this study. Furthermore, we tune the hyperparameters of each AM for each CNN separately using grid search heuristically (Sec. A1) instead of a large-scale hyperparameter search. That is, we only sweep across a limited range of values heuristically chosen from multiple rounds of tests. We choose to include WSL, Pointing Game, Deletion and Insertion, which are representative of localization-based and score-based metrics. However, some explainability conclusions may change when tested on ROAR [25], which however is not included in our work due to its excessive computational CNN-training cost at the scale of our study (i.e., testing over 9 AM methods, 12 CNNs, and 2,000 images). Therefore, we leave ROAR for future work.

In sum, our paper presents the first large-scale study of many CNNs and AM methods and finds a list of important, practical insights that are under-explored in the prior AM literature. Interestingly, PGD-1 model performing roughly the best under PG, WSL, and Insertion on ImageNet images (Fig. A9) invites future research on how to leverage AdvProp models for the actual downstream human-in-the-loop image classification tasks.

Acknowledgement

PC and AN was supported by the NSF Grant No. 1850117 & 2145767 and a donation from NaphCare Foundation. MN and LK are supported by NSF grant 1813537.

Checklist

The checklist follows the references. Please read the checklist guidelines carefully for information on how to answer these questions. For each question, change the default **[TODO]** to **[Yes]**, **[No]**, or **[N/A]**. You are strongly encouraged to include a **justification to your answer**, either by referencing the appropriate section of your paper or providing a brief inline description. For example:

- Did you include the license to the code and datasets? **[Yes]** See Section.
- Did you include the license to the code and datasets? **[No]** The code and the data are proprietary.
- Did you include the license to the code and datasets? **[N/A]**

Please do not modify the questions and only use the provided macros for your answers. Note that the Checklist section does not count towards the page limit. In your paper, please delete this instructions block and only keep the Checklist section heading above along with the questions/answers below.

1. For all authors...
 - (a) Do the main claims made in the abstract and introduction accurately reflect the paper's contributions and scope? **[Yes]** The main claims in the abstract and introduction has been demonstrated in Sec. 3.
 - (b) Did you describe the limitations of your work? **[Yes]** Please see Sec. 5.
 - (c) Did you discuss any potential negative societal impacts of your work? **[N/A]**
 - (d) Have you read the ethics review guidelines and ensured that your paper conforms to them? **[Yes]**
2. If you are including theoretical results...
 - (a) Did you state the full set of assumptions of all theoretical results? **[N/A]**
 - (b) Did you include complete proofs of all theoretical results? **[N/A]**
3. If you ran experiments...
 - (a) Did you include the code, data, and instructions needed to reproduce the main experimental results (either in the supplemental material or as a URL)? **[Yes]**
 - (b) Did you specify all the training details (e.g., data splits, hyperparameters, how they were chosen)? **[Yes]**
 - (c) Did you report error bars (e.g., with respect to the random seed after running experiments multiple times)? **[Yes]**
 - (d) Did you include the total amount of compute and the type of resources used (e.g., type of GPUs, internal cluster, or cloud provider)? **[Yes]** Please see Sec. 2.5.
4. If you are using existing assets (e.g., code, data, models) or curating/releasing new assets...
 - (a) If your work uses existing assets, did you cite the creators? **[Yes]**
 - (b) Did you mention the license of the assets? **[No]** We used code and data set that are available to the public.
 - (c) Did you include any new assets either in the supplemental material or as a URL? **[No]**
 - (d) Did you discuss whether and how consent was obtained from people whose data you're using/curating? **[N/A]**
 - (e) Did you discuss whether the data you are using/curating contains personally identifiable information or offensive content? **[Yes]** We ensured that the data we used did not consist of any personally identifiable information or offensive content.
5. If you used crowdsourcing or conducted research with human subjects...
 - (a) Did you include the full text of instructions given to participants and screenshots, if applicable? **[N/A]**
 - (b) Did you describe any potential participant risks, with links to Institutional Review Board (IRB) approvals, if applicable? **[N/A]**
 - (c) Did you include the estimated hourly wage paid to participants and the total amount spent on participant compensation? **[N/A]**

References

- [1] Agarwal, C. and Nguyen, A. Explaining image classifiers by removing input features using generative models. In *Proceedings of the Asian Conference on Computer Vision*, 2020.
- [2] Agarwal, C., Nguyen, A., and Schonfeld, D. Improving robustness to adversarial examples by encouraging discriminative features. In *2019 IEEE International Conference on Image Processing (ICIP)*, pp. 3801–3505. IEEE, 2019.
- [3] Alcorn, M. A., Li, Q., Gong, Z., Wang, C., Mai, L., Ku, W.-S., and Nguyen, A. Strike (with) a pose: Neural networks are easily fooled by strange poses of familiar objects. In *Proceedings of the IEEE/CVF Conference on Computer Vision and Pattern Recognition*, pp. 4845–4854, 2019.
- [4] Arras, L., Montavon, G., Müller, K.-R., and Samek, W. Explaining recurrent neural network predictions in sentiment analysis. *EMNLP 2017*, pp. 159, 2017.
- [5] Bansal, N., Agarwal, C., and Nguyen, A. Sam: The sensitivity of attribution methods to hyperparameters. In *Proceedings of the IEEE/CVF Conference on Computer Vision and Pattern Recognition*, pp. 8673–8683, 2020.
- [6] Bau, D., Zhou, B., Khosla, A., Oliva, A., and Torralba, A. Network dissection: Quantifying interpretability of deep visual representations. In *Proceedings of the IEEE conference on computer vision and pattern recognition*, pp. 6541–6549, 2017.
- [7] Beyer, L., Hénaff, O. J., Kolesnikov, A., Zhai, X., and Oord, A. v. d. Are we done with imagenet? *arXiv preprint arXiv:2006.07159*, 2020.
- [8] Chattopadhyay, A., Sarkar, A., Howlader, P., and Balasubramanian, V. N. Grad-cam++: Generalized gradient-based visual explanations for deep convolutional networks. In *2018 IEEE Winter Conference on Applications of Computer Vision (WACV)*, pp. 839–847. IEEE, 2018.
- [9] Chen, P., Agarwal, C., and Nguyen, A. The shape and simplicity biases of adversarially robust imagenet-trained cnns. *arXiv preprint arXiv:2006.09373*, 2020.
- [10] Choe, J., Oh, S. J., Lee, S., Chun, S., Akata, Z., and Shim, H. Evaluating weakly supervised object localization methods right. In *Proceedings of the IEEE/CVF Conference on Computer Vision and Pattern Recognition*, pp. 3133–3142, 2020.
- [11] Choe, J., Oh, S. J., Lee, S., Chun, S., Akata, Z., and Shim, H. Evaluating weakly supervised object localization methods right. In *Conference on Computer Vision and Pattern Recognition (CVPR)*, 2020. to appear.
- [12] DeYoung, J., Jain, S., Rajani, N. F., Lehman, E., Xiong, C., Socher, R., and Wallace, B. C. ERASER: A benchmark to evaluate rationalized NLP models. In *Proceedings of the 58th Annual Meeting of the Association for Computational Linguistics*, pp. 4443–4458, Online, July 2020. Association for Computational Linguistics. doi: 10.18653/v1/2020.acl-main.408. URL <https://www.aclweb.org/anthology/2020.acl-main.408>.
- [13] Doshi-Velez, F. and Kim, B. Towards a rigorous science of interpretable machine learning. *arXiv preprint arXiv:1702.08608*, 2017.
- [14] Doshi-Velez, F., Kortz, M., Budish, R., Bavitz, C., Gershman, S., O’Brien, D., Schieber, S., Waldo, J., Weinberger, D., and Wood, A. Accountability of ai under the law: The role of explanation. *arXiv preprint arXiv:1711.01134*, 2017.
- [15] Erion, G., Janizek, J. D., Sturmfels, P., Lundberg, S. M., and Lee, S.-I. Improving performance of deep learning models with axiomatic attribution priors and expected gradients. *Nature machine intelligence*, 3(7):620–631, 2021.
- [16] Etmann, C., Lunz, S., Maass, P., and Schönlieb, C.-B. On the connection between adversarial robustness and saliency map interpretability. *arXiv preprint arXiv:1905.04172*, 2019.
- [17] Fong, R., Patrick, M., and Vedaldi, A. Understanding deep networks via extremal perturbations and smooth masks. In *Proceedings of the IEEE/CVF International Conference on Computer Vision*, pp. 2950–2958, 2019.
- [18] Fong, R. C. and Vedaldi, A. Interpretable explanations of black boxes by meaningful perturbation. In *Proceedings of the IEEE International Conference on Computer Vision*, pp. 3429–3437, 2017.

- [19] Fong, R. C. and Vedaldi, A. facebookresearch/torchray: Understanding deep networks via extremal perturbations and smooth masks. <https://github.com/facebookresearch/TorchRay>, 2019. (Accessed on 12/2/2021).
- [20] Gevaert, A., Rousseau, A.-J., Becker, T., Valkenborg, D., De Bie, T., and Saeys, Y. Evaluating feature attribution methods in the image domain. *arXiv preprint arXiv:2202.12270*, 2022.
- [21] Gildenblat, J. Pytorch implementation of interpretable explanations of black boxes by meaningful perturbation. <https://github.com/jacobgil/pytorch-explain-black-box>, 2021.
- [22] Gomez, T., Fréour, T., and Mouchère, H. Metrics for saliency map evaluation of deep learning explanation methods. *arXiv preprint arXiv:2201.13291*, 2022.
- [23] Hai Phan, A. N. Deepface-emd: Re-ranking using patch-wise earth mover’s distance improves out-of-distribution face identification. In *Proceedings of the IEEE/CVF Conference on Computer Vision and Pattern Recognition*, 2022.
- [24] He, K., Zhang, X., Ren, S., and Sun, J. Deep residual learning for image recognition. In *Proceedings of the IEEE conference on computer vision and pattern recognition*, pp. 770–778, 2016.
- [25] Hooker, S., Erhan, D., Kindermans, P.-J., and Kim, B. A benchmark for interpretability methods in deep neural networks. *Advances in neural information processing systems*, 32, 2019.
- [26] Huang, G., Liu, Z., Van Der Maaten, L., and Weinberger, K. Q. Densely connected convolutional networks. In *Proceedings of the IEEE conference on computer vision and pattern recognition*, pp. 4700–4708, 2017.
- [27] Jacovi, A. and Goldberg, Y. Aligning faithful interpretations with their social attribution. *Transactions of the Association for Computational Linguistics*, 9:294–310, 2021.
- [28] Kim, S., Yi, J., Kim, E., and Yoon, S. Interpretation of NLP models through input marginalization. In *Proceedings of the 2020 Conference on Empirical Methods in Natural Language Processing (EMNLP)*, pp. 3154–3167, Online, November 2020. Association for Computational Linguistics. doi: 10.18653/v1/2020.emnlp-main.255. URL <https://www.aclweb.org/anthology/2020.emnlp-main.255>.
- [29] Kokhlikyan, N., Miglani, V., Martin, M., Wang, E., Alsallakh, B., Reynolds, J., Melnikov, A., Kliushkina, N., Araya, C., Yan, S., and Reblitz-Richardson, O. Captum: A unified and generic model interpretability library for pytorch, 2020.
- [30] Krizhevsky, A., Sutskever, I., and Hinton, G. E. Imagenet classification with deep convolutional neural networks. *Advances in neural information processing systems*, 25:1097–1105, 2012.
- [31] Lapuschkin, S., Binder, A., Montavon, G., Müller, K.-R., and Samek, W. Analyzing classifiers: Fisher vectors and deep neural networks. In *Proceedings of the IEEE Conference on Computer Vision and Pattern Recognition*, pp. 2912–2920, 2016.
- [32] Lipton, Z. C. The doctor just won’t accept that! *arXiv preprint arXiv:1711.08037*, 2017.
- [33] Lundberg, S. and Lee, S.-I. A unified approach to interpreting model predictions. *arXiv preprint arXiv:1705.07874*, 2017.
- [34] Lundberg, S. M. and Lee, S.-I. A unified approach to interpreting model predictions. In Guyon, I., Luxburg, U. V., Bengio, S., Wallach, H., Fergus, R., Vishwanathan, S., and Garnett, R. (eds.), *Advances in Neural Information Processing Systems 30*, pp. 4765–4774. Curran Associates, Inc., 2017. URL <http://papers.nips.cc/paper/7062-a-unified-approach-to-interpreting-model-predictions.pdf>.
- [35] Madry, A., Makelov, A., Schmidt, L., Tsipras, D., and Vladu, A. Towards deep learning models resistant to adversarial attacks. *arXiv preprint arXiv:1706.06083*, 2017.
- [36] Nguyen, A., Yosinski, J., and Clune, J. Deep neural networks are easily fooled: High confidence predictions for unrecognizable images. In *Proceedings of the 2015 IEEE Conference on Computer Vision and Pattern Recognition (CVPR)*, CVPR ’15, pp. 427–436. IEEE, June 2015. doi: 10.1109/CVPR.2015.7298640.
- [37] Noack, A., Ahern, I., Dou, D., and Li, B. An empirical study on the relation between network interpretability and adversarial robustness. *SN Computer Science*, 2(1):1–13, 2021.
- [38] Petsiuk, V. Randomized input sampling for explanation of black-box models. <https://github.com/eclique/RISE>, 2018. (Accessed on 12/2/2021).
- [39] Petsiuk, V., Das, A., and Saenko, K. Rise: Randomized input sampling for explanation of black-box models. *arXiv preprint arXiv:1806.07421*, 2018.

- [40] Pham, T. M., Bui, T., Mai, L., and Nguyen, A. Double trouble: How to not explain a text classifier’s decisions using counterfactuals synthesized by masked language models? *arXiv preprint arXiv:2110.11929*, 2021.
- [41] Rajpurkar, P., Irvin, J., Zhu, K., Yang, B., Mehta, H., Duan, T., Ding, D., Bagul, A., Langlotz, C., Shpanskaya, K., et al. Chexnet: Radiologist-level pneumonia detection on chest x-rays with deep learning. *arXiv preprint arXiv:1711.05225*, 2017.
- [42] Ribeiro, M. T., Singh, S., and Guestrin, C. "why should I trust you?": Explaining the predictions of any classifier. In *Proceedings of the 22nd ACM SIGKDD International Conference on Knowledge Discovery and Data Mining, San Francisco, CA, USA, August 13-17, 2016*, pp. 1135–1144, 2016.
- [43] Ribeiro, M. T., Singh, S., and Guestrin, C. " why should i trust you?" explaining the predictions of any classifier. In *Proceedings of the 22nd ACM SIGKDD international conference on knowledge discovery and data mining*, pp. 1135–1144, 2016.
- [44] Ross, A. and Doshi-Velez, F. Improving the adversarial robustness and interpretability of deep neural networks by regularizing their input gradients. In *Proceedings of the AAAI Conference on Artificial Intelligence*, volume 32, 2018.
- [45] Russakovsky, O., Deng, J., Su, H., Krause, J., Satheesh, S., Ma, S., Huang, Z., Karpathy, A., Khosla, A., Bernstein, M., et al. Imagenet large scale visual recognition challenge. *International journal of computer vision*, 115(3):211–252, 2015.
- [46] Samek, W., Binder, A., Montavon, G., Lapuschkin, S., and Müller, K.-R. Evaluating the visualization of what a deep neural network has learned. *IEEE transactions on neural networks and learning systems*, 28(11):2660–2673, 2016.
- [47] Sandler, M., Howard, A., Zhu, M., Zhmoginov, A., and Chen, L.-C. Mobilenetv2: Inverted residuals and linear bottlenecks. In *Proceedings of the IEEE conference on computer vision and pattern recognition*, pp. 4510–4520, 2018.
- [48] Selvaraju, R. R., Cogswell, M., Das, A., Vedantam, R., Parikh, D., and Batra, D. Grad-cam: Visual explanations from deep networks via gradient-based localization. In *Proceedings of the IEEE international conference on computer vision*, pp. 618–626, 2017.
- [49] Simonyan, K. and Zisserman, A. Very deep convolutional networks for large-scale image recognition. *arXiv preprint arXiv:1409.1556*, 2014.
- [50] Simonyan, K., Vedaldi, A., and Zisserman, A. Deep inside convolutional networks: Visualising image classification models and saliency maps. *arXiv preprint arXiv:1312.6034*, 2013.
- [51] Smilkov, D., Thorat, N., Kim, B., Viégas, F., and Wattenberg, M. Smoothgrad: removing noise by adding noise. *arXiv preprint arXiv:1706.03825*, 2017.
- [52] Sovrasov, V. Flops counter for convolutional networks in pytorch framework. <https://github.com/sovrasov/flops-counter.pytorch>, 2019. (Accessed on 03/29/2022).
- [53] Sundararajan, M., Taly, A., and Yan, Q. Axiomatic attribution for deep networks. In *International Conference on Machine Learning*, pp. 3319–3328. PMLR, 2017.
- [54] Szegedy, C., Liu, W., Jia, Y., Sermanet, P., Reed, S., Anguelov, D., Erhan, D., Vanhoucke, V., and Rabinovich, A. Going deeper with convolutions. In *Proceedings of the IEEE conference on computer vision and pattern recognition*, pp. 1–9, 2015.
- [55] Tomsett, R., Harborne, D., Chakraborty, S., Gurram, P., and Preece, A. Sanity checks for saliency metrics. In *Proceedings of the AAAI conference on artificial intelligence*, volume 34, pp. 6021–6029, 2020.
- [56] Xie, C., Tan, M., Gong, B., Wang, J., Yuille, A. L., and Le, Q. V. Adversarial examples improve image recognition. In *Proceedings of the IEEE/CVF Conference on Computer Vision and Pattern Recognition*, pp. 819–828, 2020.
- [57] Yin, D., Gontijo Lopes, R., Shlens, J., Cubuk, E. D., and Gilmer, J. A fourier perspective on model robustness in computer vision. *Advances in Neural Information Processing Systems*, 32, 2019.
- [58] Zhang, H., Yu, Y., Jiao, J., Xing, E., El Ghaoui, L., and Jordan, M. Theoretically principled trade-off between robustness and accuracy. In *International conference on machine learning*, pp. 7472–7482. PMLR, 2019.

- [59] Zhang, J., Bargal, S. A., Lin, Z., Brandt, J., Shen, X., and Sclaroff, S. Top-down neural attention by excitation backprop. *International Journal of Computer Vision*, 126(10):1084–1102, 2018.
- [60] Zhang, T. and Zhu, Z. Interpreting adversarially trained convolutional neural networks. In *International Conference on Machine Learning*, pp. 7502–7511. PMLR, 2019.
- [61] Zhou, B., Khosla, A., Lapedriza, A., Oliva, A., and Torralba, A. Learning deep features for discriminative localization. In *Proceedings of the IEEE conference on computer vision and pattern recognition*, pp. 2921–2929, 2016.

Appendix for: How explainable are adversarially-robust CNNs?

A1 Hyperparameter settings

A1.1 Hyperparameter tuning

Most gradient-based and CAM-based methods do not have hyperparameters while perturbation-based methods are often the most beneficial from hyperparameter tuning (Table A1).

Several of the attribution methods we consider here have hyperparameters that affect their behavior. For **IG**, Captum [29] suggests $N_{steps} = 50$ and for **SHAP** [34] the default is $N_{samples} = 200$. The defaults for **MP** [21] are $\beta = 3$, learning rate $\gamma = 0.1$, 500 iterations, $\lambda_1 = 0.01$, and $\lambda_2 = 0.2$. For **EP** [19], default hyperparameters are areas = [0.025, 0.05, 0.1, 0.2], 800 iterations, and smoothing = 0.09. For **RISE** [39], $N_{masks} = 8000$ and mask size = 7. And for **LIME** [42], $N_{samples} = 1000$, $N_{superpixels} = 50$.

The default or suggested hyperparameters in the literature were tuned for vanilla CNNs; the optimal values are not necessarily the same for robust CNNs. We tuned the hyperparameters for perturbation-based methods across all CNNs. We use 250 randomly chosen images from ImageNet [45] that are not in ImageNet-CL. Then we define the search space as mentioned in the following paragraph and perform a grid search over all these hyperparameters for the best performance.

EP We sweep across the following lists of “area sizes”: { [0.05, 0.1], [0.02, 0.08, 0.16], [0.05, 0.15, 0.3], [0.025, 0.05, 0.1, 0.2], [0.012, 0.025, 0.05, 0.1, 0.2], [0.012, 0.025, 0.05, 0.1, 0.2, 0.4], [0.015, 0.03, 0.05, 0.1, 0.25, 0.5], [0.01, 0.04, 0.05, 0.1, 0.2, 0.4] }.

MP We sweep across the following numbers of steps: { 5, 10, 25, 50, 100, 200, 300, 400, 500 }.

RISE We sweep across different numbers of masks: { 100, 200, 400, 600, 800, 1000, 2000, 3000, 4000, 5000, 6000, 7000, 8000, 9000, 10000 } and the different values for the mask size: { 3, 4, 5, 6, 7, 8, 9 }.

LIME We sweep across the following values for the numbers of superpixels: { 10, 20, 30, 40, 50, 60 }. Changing the number of samples shows no significant effect on LIME explanation accuracy, so we do not tune this hyperparameter.

A1.2 Best hyperparameter settings

As the result of tuning, below are the final hyperparameter settings for each method used in the paper.

EP Implementation: https://facebookresearch.github.io/TorchRay/attribution.html#module-torchray.attribution.extremal_perturbation

- Iterations = 800
- Smoothing = 0.09
- reward function = simple reward
- Perturbation = 'blur'

Table A1: Best hyperparameters for each network and method. **Bold** numbers are the hyperparameter values found that are better than the default settings.

	EP [17] Area sizes	MP [18] Number of steps	RISE [39] Mask size, number of samples	LIME [43] Number of superpixels
<i>Default</i>	[0.025, 0.05, 0.1, 0.2]	500	7, 8000	50
AlexNet	[0.012, 0.025, 0.05, 0.1, 0.2]	500	7, 8000	40
AlexNet-R	[0.015, 0.03, 0.05, 0.1, 0.25, 0.5]	10	3, 4000	20
GoogLeNet	[0.025, 0.05, 0.1, 0.2]	500	7, 8000	40
GoogLeNet-R	[0.025, 0.05, 0.1, 0.2]	10	3, 8000	40
ResNet	[0.025, 0.05, 0.1, 0.2]	500	7, 8000	50
ResNet-R	[0.025, 0.05, 0.1, 0.2]	10	4, 7000	20
MobileNet	[0.025, 0.05, 0.1, 0.2]	400	6, 7000	40
MobileNet-R	[0.025, 0.05, 0.1, 0.2]	10	4, 8000	20
DenseNet	[0.025, 0.05, 0.1, 0.2]	500	7, 8000	50
DenseNet-R	[0.025, 0.05, 0.1, 0.2]	10	4, 7000	50
PGD-5	[0.025, 0.05, 0.1, 0.2]	500	7, 8000	50
PGD-1	[0.025, 0.05, 0.1, 0.2]	500	7, 8000	40

- Step = 7
- Sigma = 21
- Jitter = True
- Areas sizes : see Table A1

MP Implementation: <https://github.com/jacobgil/pytorch-explain-black-box>

- $\beta = 3$
- learning rate $\gamma = 0.1$
- Iterations = 500
- $\lambda_1 = 0.01$
- $\lambda_2 = 0.2$
- Number of steps : see Table A1

RISE Implementation: <https://github.com/eclique/RISE>

- probability of producing 1s in the binary masks = 0.5
- Mask and Number of samples : see Table A1

LIME Implementation: <https://github.com/marcotcr/lime/blob/master/doc/notebooks/Tutorial%20-%20images%20-%20Pytorch.ipynb>

- Number of samples = 1000
- Segmenter parameters:
Compactness = 10
Sigma = 3
- Number of superpixels : see Table A1

SHAP Implementation: <https://shap-lrjball.readthedocs.io/en/latest/generated/shap.GradientExplainer.html>

- Number of samples = 200

IG Implementation: https://captum.ai/api/integrated_gradients.html

- Number of steps = 50

Gradient Implementation: <https://facebookresearch.github.io/TorchRay/attribution.html#module-torchray.attribution.gradient>

GradCAM Implementation: <https://github.com/jacobgil/pytorch-grad-cam>

CAM Implementation: <https://github.com/zhoubolei/CAM>

A2 ImageNet-CL results continuation

A2.1 ResNet-50’s explanations outperform other architectures on average

We used five different architectures as described in Sec. 2.2 for our experiments. We want to know which architecture would have the best performance overall. To the best of our knowledge, we are the first one to compare architectures explainability wise.

Experiment Given the experiment in Sec. 3.1, we consider each architecture (including vanilla and robust CNNs) across our nine attribution methods on ImageNet-CL data set. For each metric, we draw the boxplot of each architecture (excluding AdvProp networks to have a fair comparison of architectures since other architectures only consist of robust and vanilla). Fig. A1 depicts the ranking of the explanations derived from different architectures as the average over robust and vanilla networks and eight attribution methods(excluding CAM) across our four metrics.

Result Fig. A1 shows that ResNet-50 is the best architecture considering the average rankings of architectures summarized in Table A5. GoogLeNet and DenseNet-161 are two competitive architectures after ResNet-50 while MobileNet-v2 and AlexNet are the worst architectures overall. Even though ResNet-50 is the best overall, it is one to the last in Deletion. In the same vein, AlexNet is the best in Deletion but is the worst in both localization metrics, i.e. WSL and pointing game.

Furthermore, the ImageNet results regarding ranking architectures depicted in Fig. A7 show the same set of conclusion as ImageNet-CL regarding architectures, e.g. ResNet-50 and AlexNet on average are the best and the worst architectures, respectively.

Our finding suggests that architectures with higher test-set accuracy do not necessarily have better explainability scores; Even though DenseNet-161 has the higher average accuracy, it is not the best architecture across our evaluation metrics on average (see Table A5).

Recommendation We recommend ML practitioners to use ResNet-50 architecture since it is the best compromise between top-1 classification accuracy and explainability compared to other architectures.

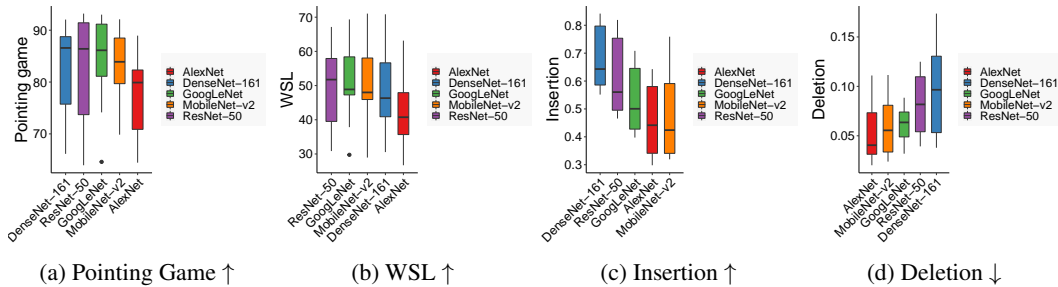


Figure A1: (a)-(d) show the average performances of our five architectures methods in Sec. 2.2 across eight attribution methods in Sec. 2.3 (excluding CAM) for pointing game, WSL, Insertion, and Deletion, respectively. RestNet-50 is the best overall and MP is the worst.(see Table A5). Interestingly, high top-1 accuracy

A2.2 CNNs ranking for Pointing Game and Deletion

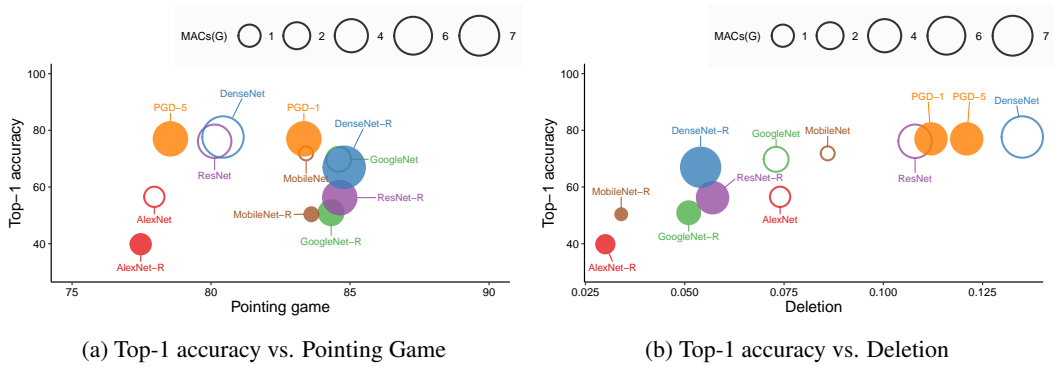


Figure A2: Shows the average performance of all CNNs across eight attribution methods for Pointing Game and Deletion along with top-1 accuracy and MACs. See Fig. 5 for the same plot for WSL and Insertion.

A2.3 Insertion and Deletion examples to show the bias of these two metrics

This section is an extension for Fig. 6a to demonstrate for the bias of Insertion and Deletion.

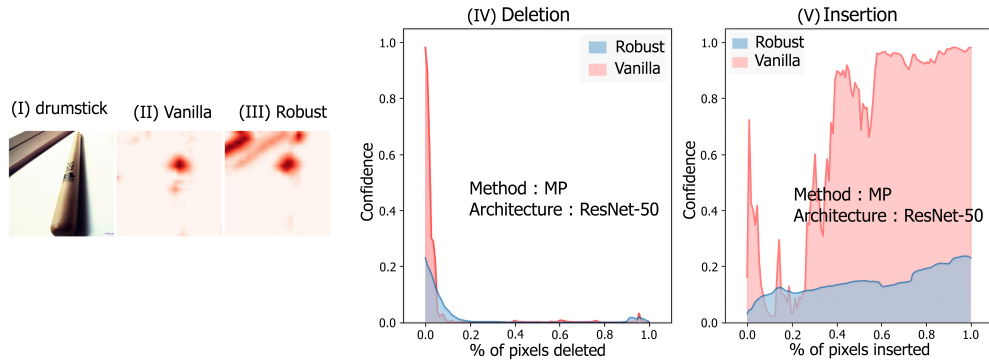


Figure A3: Given the same “drumstick” image (I), the MP heatmaps of ResNet and ResNet-R are not of good quality. Yet, under Deletion (robust AUC = 0.01 vs. vanilla AUC=0.03), the robust heatmap (III) is better. In contrast, under Insertion, the vanilla heatmap (II) is better.

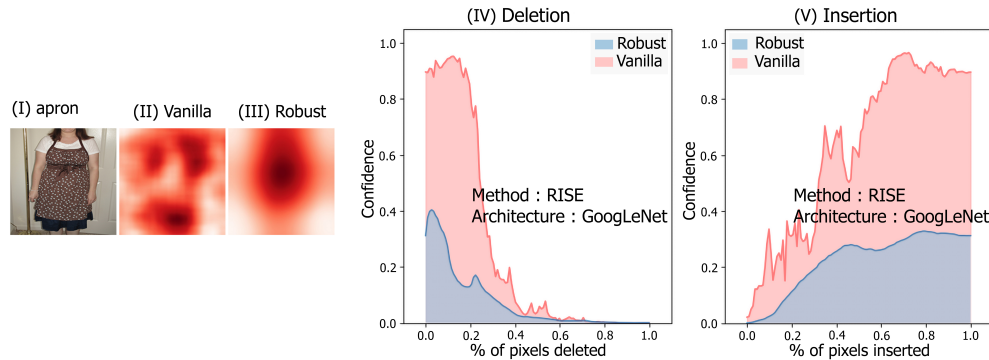


Figure A4: Given the same “apron” image (I), the RISE heatmaps of GoogleNet and GooleNet-R are shown in (II) and (III), respectively. Again as we saw in Fig. A3, under Deletion, the robust heatmap (III) is better. In contrast, under Insertion, the vanilla heatmap (II) is better.

A3 Rankings of methods, architectures and networks

Table A2: Mean \pm std and ranking of AM methods as shown in Fig. 4 over all CNNs shown in bold on **ImageNet-CL**. Average of rankings is the mean value of rankings across the evaluation metrics.

	Pointing game	WSL	Insertion	Deletion	Average of rankings
GradCAM	85.32 \pm 10.19 (3rd)	62.29 \pm 14.17 (1st)	0.57 \pm 0.19 (2nd)	0.07 \pm 0.03 (3rd)	2.25
RISE	91.41 \pm 1.87 (1st)	56.72 \pm 7.03 (3rd)	0.57 \pm 0.19 (2nd)	0.07 \pm 0.03 (3rd)	2.25
EP	89.70 \pm 2.07 (2nd)	59.06 \pm 2.53 (2nd)	0.59 \pm 0.19 (1st)	0.08 \pm 0.04 (6th)	2.75
IG	82.24 \pm 4.84 (4th)	44.97 \pm 4.23 (6th)	0.53 \pm 0.12 (6th)	0.06 \pm 0.03 (2nd)	4.5
SHAP	81.91 \pm 4.81 (5th)	42.61 \pm 6.63 (7th)	0.53 \pm 0.12 (6th)	0.05 \pm 0.03 (1st)	4.75
LIME	78.01 \pm 4.36 (7th)	45.47 \pm 2.91 (5th)	0.56 \pm 0.19 (4th)	0.07 \pm 0.03 (3rd)	4.75
Gradient	78.36 \pm 7.81 (6th)	47.03 \pm 6.88 (4th)	0.50 \pm 0.11 (8th)	0.08 \pm 0.04 (6th)	6
MP	70.14 \pm 3.51 (8th)	31.58 \pm 3.12 (8th)	0.56 \pm 0.14 (4th)	0.08 \pm 0.03 (6th)	6.5

Table A3: Mean \pm std and ranking of AM methods as shown in Fig. A8 over all CNNs shown in bold on **ImageNet**. Average of rankings is the mean value of rankings across our four evaluation metrics.

	Pointing game	WSL	Insertion	Deletion	Average of rankings
EP	84.63 \pm 4.04 (1st)	47.42 \pm 3.16 (2nd)	0.34 \pm 0.17 (2nd)	0.04 \pm 0.02 (3rd)	2
RISE	82.20 \pm 7.65 (2nd)	42.62 \pm 5.95 (3rd)	0.36 \pm 0.18 (1st)	0.04 \pm 0.02 (3rd)	2.25
GradCAM	77.95 \pm 10.35 (3rd)	51.63 \pm 11.82 (1st)	0.33 \pm 0.17 (3rd)	0.04 \pm 0.02 (3rd)	2.5
IG	77.14 \pm 4.14 (4th)	38.34 \pm 3.71 (5th)	0.30 \pm 0.12 (6th)	0.03 \pm 0.02 (1st)	4
SHAP	76.85 \pm 3.80 (5th)	36.43 \pm 5.31 (6th)	0.30 \pm 0.12 (6th)	0.03 \pm 0.02 (1st)	4.5
LIME	67.07 \pm 7.64 (7th)	35.07 \pm 4.93 (7th)	0.33 \pm 0.17 (3rd)	0.04 \pm 0.02 (3rd)	5
Gradient	74.04 \pm 7.09 (6th)	40.43 \pm 5.30 (4th)	0.28 \pm 0.11 (8th)	0.05 \pm 0.03 (7th)	6.25
MP	65.61 \pm 5.64 (8th)	25.72 \pm 3.93 (8th)	0.33 \pm 0.15 (3rd)	0.05 \pm 0.02 (7th)	6.5

Table A4: Ranking of CNNs considering under all evaluation metrics, top-1 accuracy, and MACs on **ImageNet-CL**.

	Pointing game	WSL	Insertion	Deletion	Top-1 accuracy	MACs (G)
AlexNet	77.96 (11th)	43.81 (11th)	0.582 (7th)	0.074 (7th)	56.55 (8th)	0.72 (3rd)
AlexNet-R	77.47 (12th)	41.78 (12th)	0.333 (12th)	0.03 (1st)	39.83 (12th)	0.72 (3rd)
GoogleNet	84.59 (3rd)	50.9 (4th)	0.632 (5th)	0.073 (6th)	69.78 (6th)	1.51 (5th)
GoogleNet-R	84.32 (4th)	52.59 (2nd)	0.428 (10th)	0.051 (3rd)	50.94 (10th)	1.51 (5th)
DenseNet	80.43 (8th)	45.67 (10th)	0.78 (2nd)	0.135 (12th)	77.14 (2nd)	7.82 (11th)
DenseNet-R	84.79 (1st)	52.06 (3rd)	0.579 (8th)	0.054 (4th)	66.12 (7th)	7.82 (11th)
MobileNet	83.42 (6th)	50.31 (6th)	0.611 (6th)	0.086 (8th)	71.88 (5th)	0.32 (1st)
MobileNet-R	83.61 (5th)	50.65 (5th)	0.338 (11th)	0.034 (2nd)	50.4 (11th)	0.32 (1st)
ResNet	80.13 (9th)	46.11 (9th)	0.727 (4th)	0.108 (9th)	76.15 (4th)	4.12 (9th)
ResNet-R	84.63 (2nd)	53.27 (1st)	0.496 (9th)	0.057 (5th)	56.25 (9th)	4.12 (9th)
PGD-5	78.54 (10th)	48.07 (8th)	0.796 (1st)	0.121 (11th)	77.01 (3rd)	4.1 (7th)
PGD-1	83.34 (7th)	50.11 (7th)	0.778 (3rd)	0.112 (10th)	77.31 (1st)	4.1 (7th)

Table A5: Median (interquartile range) and architectures' rank (bold) shown in Fig. A1 for each metric on **ImageNet-CL**. Average of rankings is the mean value of rankings across the evaluation metrics.

	Pointing Game	WSL	Insertion	Deletion	Average of rankings
ResNet-50	86.40 (17.71), 2nd	51.75 (18.40), 1st	0.56 (0.26), 2nd	0.08 (0.06), 4th	2.25
GoogLeNet	86.13 (10.05), 3rd	48.88 (11.13), 2nd	0.50 (0.22), 3rd	0.06 (0.03), 3rd	2.75
DenseNet-161	86.58 (13.01), 1st	46.33 (15.76), 4th	0.64 (0.21), 1st	0.10 (0.08), 5th	2.75
MobileNet	83.90 (8.80), 4th	48.00 (12.14), 3rd	0.42 (0.25), 5th	0.06 (0.05), 2nd	3.5
AlexNet	79.90 (11.45), 5th	40.75 (12.25), 5th	0.44 (0.24), 4th	0.04 (0.04), 1st	3.75

A4 Results and analysis of ImageNet

In this section, we explain the results that have been obtained by using ImageNet defined in Sec. 2.1 in comparison with ImageNet-CL results demonstrated in Sec. 3.

A4.1 Robust models outperform their vanilla counterpart in gradient-based methods

As we can see in Fig. A5, we reach the same conclusion as in Sec. 3.1 for CAM-based and Gradient-based methods as we previously saw for ImageNet-CL. The only difference is about Perturbation-based methods, in which we see vanilla models outperform robust models.

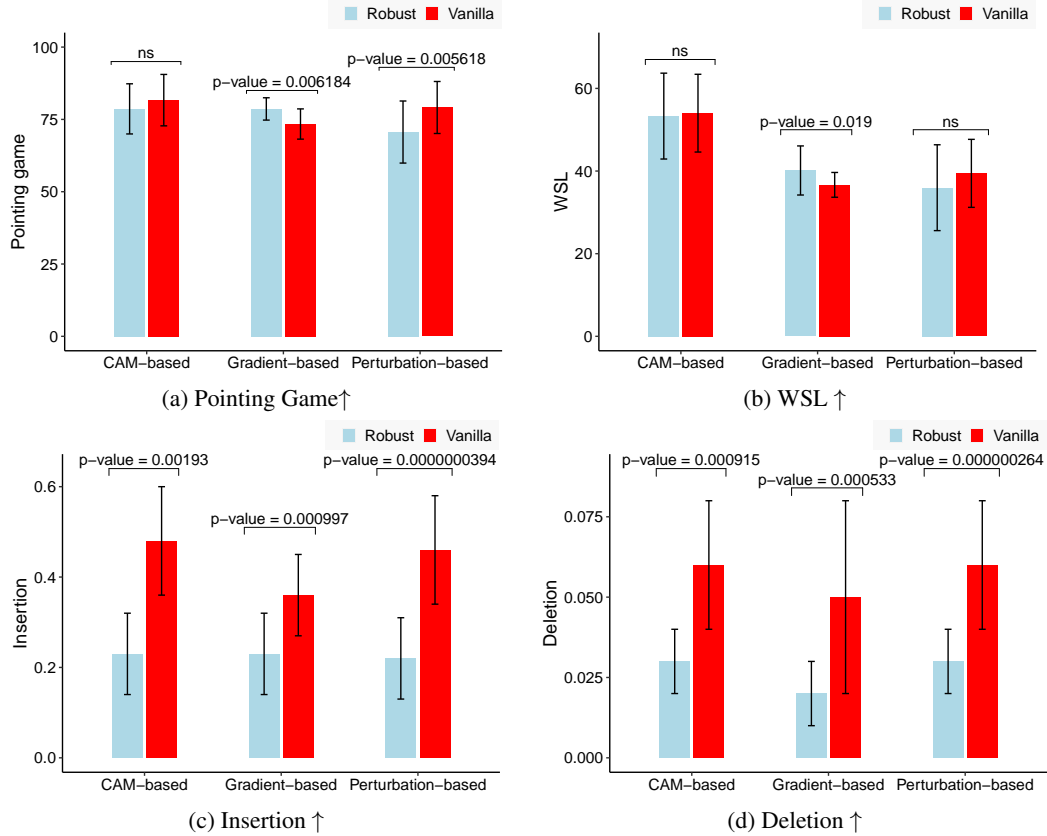


Figure A5: Performance of explanations generated from vanilla and robust models for three different types of AM methods across four different metrics on ImageNet images which are aligned with the conclusion in Sec. 3.1; Robust models outperform vanilla ones in gradient-based methods but not in CAM-based nor perturbation-based methods.

A4.2 AdvProp models outperform vanilla models in both classifiability and explainability

We also conclude the same result as we saw in Sec. 3.2 that an incremental trend is visible from vanilla to robust models by AdvProp models being in between, as we can see in Fig. A6 for localization metrics.

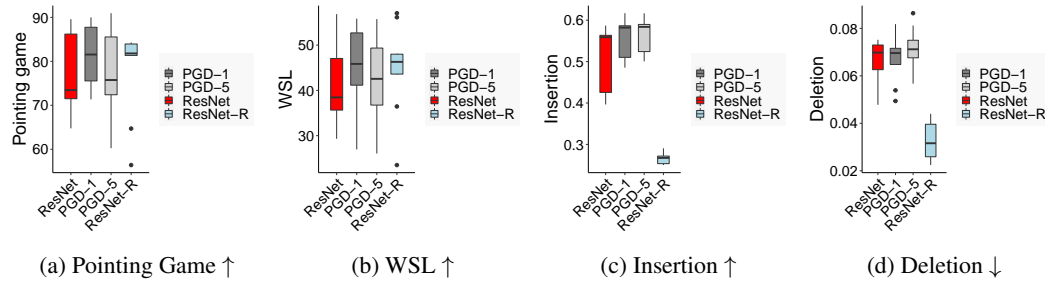


Figure A6: AdvProp models outperform vanilla models in all metrics except Deletion (d), i.e. Pointing Game (a), WSL (b), and Insertion (c). Also, as shown, it supports the smooth transition we saw in ImageNet-CL (see Fig. 3).

A4.3 ResNet-50 and DenseNet-161 are the top architecture to use

ResNet-50 is the top architecture as shown in Fig. A7, which we saw in Sec. A2.1. MobileNet-v2 and AlexNet are the best architectures in Deletion, while they are consistently the worst for the other three evaluation metrics.

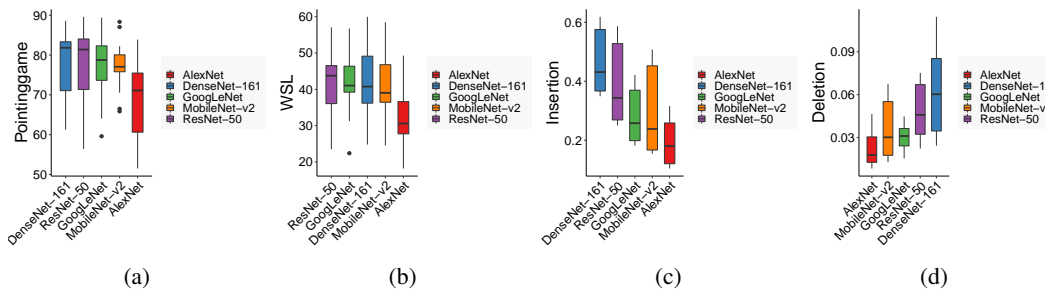


Figure A7: ResNet-50 is the overall best architecture as we concluded on ImageNet-CL before (see Sec. A2.1). Also, even though AlexNet and MobileNet-v2 are the best architectures under Deletion, they are consistently the worst across the other three metrics.

A4.4 EP, RISE, and GradCAM are the best AM methods considering all metrics

The three best AMs overall came out to be EP, RISE, and GradCAM on ImageNet (see Table A3 for average of rankings), as shown in Fig. A8. These top-3 methods are what we obtained for ImageNet-CL in Sec. 3.3.

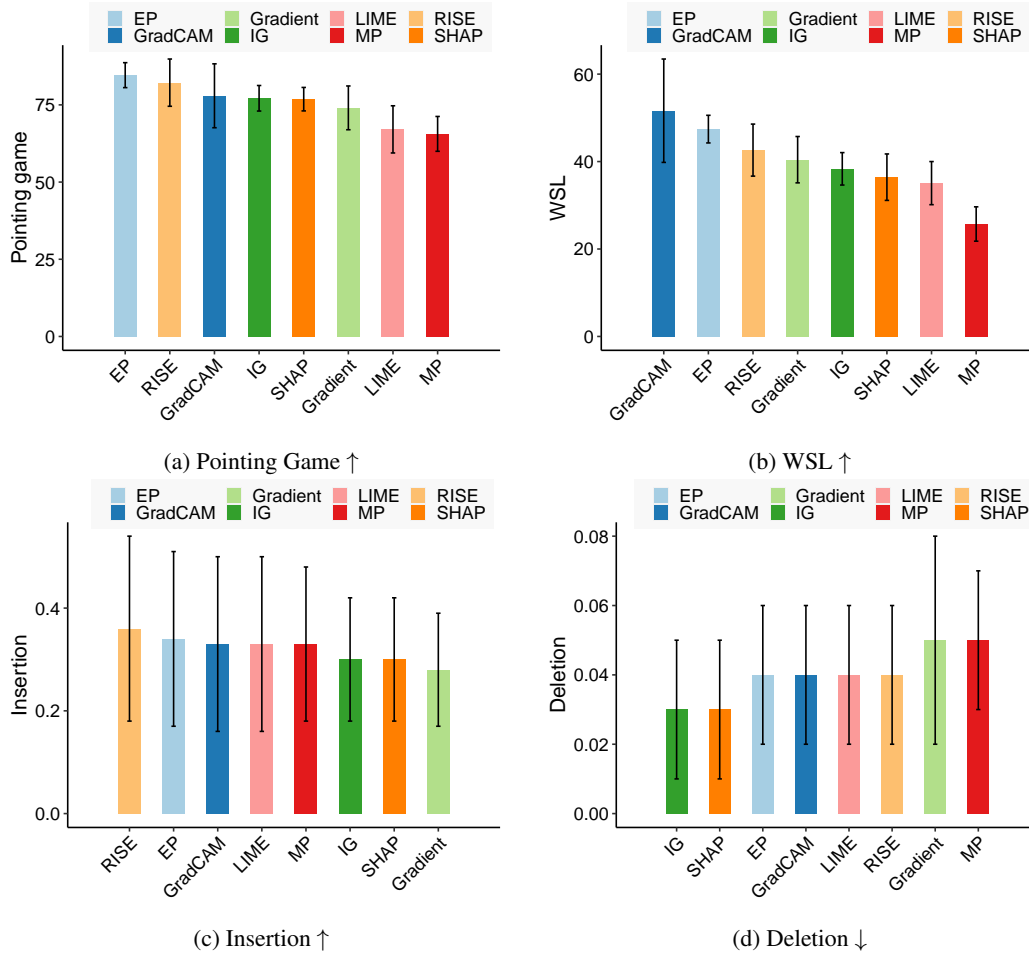


Figure A8: EP, RISE, and GradCAM are the best AM methods as they are consistently among top-3 for all metrics, which we concluded on ImageNet-CL (see Sec. 3.3) as well. Moreover, MP is the worst method as it is the last in the ranking in all metrics except Insertion (c) which is exactly the same on ImageNet-CL (see Fig. 4).

A4.5 CNN classification accuracy, explanations, and number of multiply-accumulate operations

As explained in Sec. 3.4 we find no CNNs to be the best across all evaluation metrics and criteria. Considering explanation accuracy, top-1 accuracy, and MACs, PGD-1 model is the best, as depicted in Fig. A9 on average. This is the same as what we concluded for ImageNet-CL (see Fig. 5).

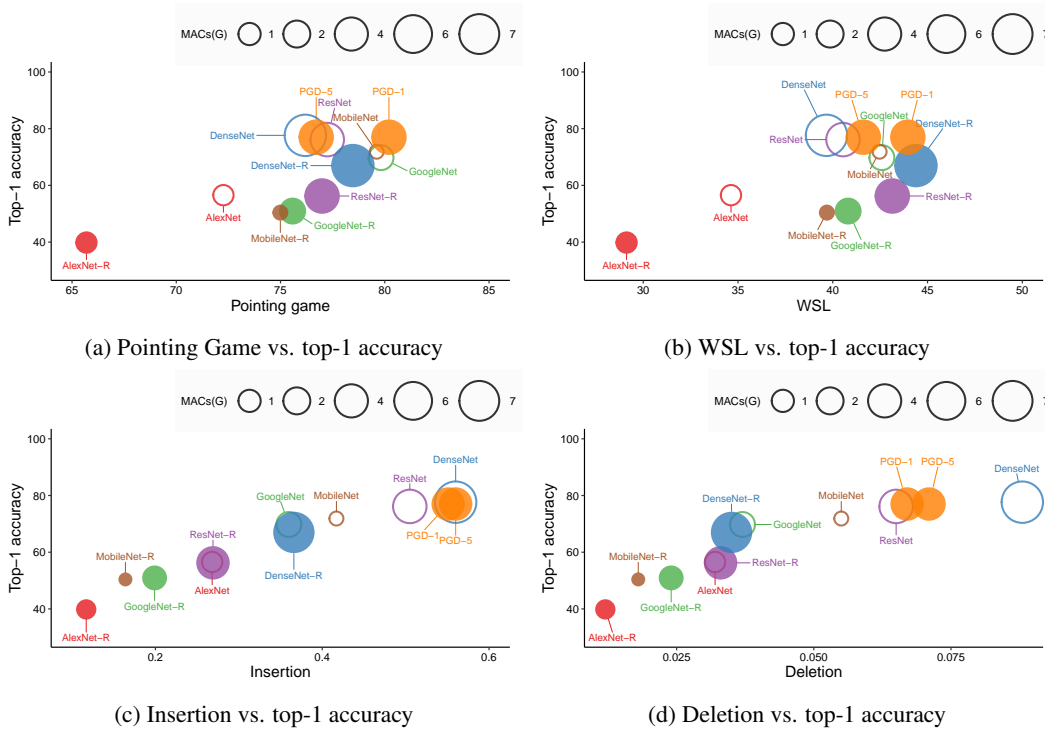


Figure A9: The average explainability score vs. MACs and top-1 accuracy show that no CNN is the best across all metrics and criteria as we stated in Sec. 3.4. However, on average, it seems that AdvProp model, i.e. PGD-1, is the best on average since it is among the best for Insertion, WSL, Pointing Game, and top-1 accuracy.

A5 Quantitative results of ImageNet-CL

In this section, the quantitative results of the experiment in Sec. 3.1 will be presented for the evaluation metrics for all CNNs and AM methods on ImageNet-CL.

Table A6: Pointing game for all 9 AM methods and 12 CNNs for experiment in Sec. 3.1 on **ImageNet-CL**. Bold numbers are the best CNNs for each AM method. In gradient-based methods, robust models are performing better by a great deal compared to their vanilla counter parts as our results in Sec. 3.1 suggests.

	Gradient-based			CAM-based		Perturbation-based			
	Gradient	IG	SHAP	GradCAM	CAM	RISE	LIME	MP	EP
AlexNet	76.50	81.55	80.70	64.45	N/A	88.55	71.35	71.60	88.95
AlexNet-R	79.85	81.30	79.95	68.25	N/A	87.60	69.45	68.70	84.65
GoogLeNet	76.40	83.15	83.20	92.65	92.65	93.00	82.10	74.15	92.10
GoogLeNet-R	85.75	86.75	86.50	90.85	90.85	92.55	78.15	64.60	89.40
ResNet	64.50	72.30	74.05	91.95	92.00	93.20	81.05	72.70	91.25
ResNet-R	86.15	86.65	87.35	91.95	91.95	92.05	78.80	63.95	90.15
MobileNet	79.05	83.05	79.90	88.40	N/A	92.10	81.20	72.45	91.20
MobileNet-R	83.25	84.55	85.05	87.95	N/A	91.00	78.50	69.85	88.75
DenseNet	66.15	75.95	75.10	88.35	88.10	91.95	82.00	73.20	90.70
DenseNet-R	86.00	87.15	87.25	88.40	85.30	92.05	77.50	70.15	89.80
PGD-5	73.15	82.75	77.10	58.80	91.10	92.15	82.50	70.65	91.20
PGD-1	75.60	84.10	79.4	89.50	92.05	92.75	82.15	72.10	91.15

Table A7: WSL for all 9 AM methods and 12 CNNs for experiment in Sec. 3.1 on **ImageNet-CL**. Bold numbers are the best CNNs for each AM method. Mostly, robust CNNs achieving the maximum score (6 out of 9 AM methods).

	Gradient-based			CAM-based		Perturbation-based			
	Gradient	IG	SHAP	GradCAM	CAM	RISE	LIME	MP	EP
AlexNet	42.95	43.90	39.95	35.30	N/A	52.95	41.55	30.70	63.15
AlexNet-R	46.25	36.70	32.85	35.80	N/A	57.35	39.80	26.70	58.80
GoogLeNet	48.30	47.45	45.05	68.65	68.70	49.25	48.65	37.85	62.00
GoogLeNet-R	52.50	48.60	49.10	69.35	69.50	67.45	46.75	29.75	57.20
ResNet	36.45	40.55	36.25	66.10	65.80	52.60	45.50	33.45	58.00
ResNet-R	54.05	51.35	52.15	67.15	67.10	65.75	46.95	30.85	57.90
MobileNet	47.25	46.25	38.85	71.05	N/A	53.45	48.75	34.25	62.65
MobileNet-R	50.55	46.10	45.40	69.15	N/A	60.65	47.20	28.95	57.20
DenseNet	35.95	42.35	36.5	69.45	65.70	46.20	44.90	32.75	57.25
DenseNet-R	56.05	46.45	50.00	70.85	69.00	61.55	44.60	30.55	56.45
PGD-5	44.90	49.60	42.35	57.30	66.15	48.45	45.85	30.15	65.95
PGD-1	48.90	51.80	45.60	61.10	66.70	50.50	45.05	33.25	64.65

Table A8: Insertion for all 9 AM methods and 12 CNNs for experiment in Sec. 3.1 on **ImageNet-CL**. Bold numbers are the best CNNs for each AM method. As we stated in Sec. 3.5, we can observe that two CNNs with the high mean confidence are dominating Insertion; PGD-5 and DenseNet.

	Gradient-based			CAM-based		Perturbation-based			
	Gradient	IG	SHAP	GradCAM	CAM	RISE	LIME	MP	EP
AlexNet	0.522	0.553	0.559	0.579	N/A	0.643	0.593	0.584	0.627
AlexNet-R	0.347	0.356	0.342	0.307	N/A	0.311	0.298	0.361	0.339
GoogLeNet	0.536	0.575	0.579	0.670	0.670	0.708	0.670	0.637	0.682
GoogLeNet-R	0.431	0.459	0.465	0.401	0.401	0.401	0.397	0.453	0.419
ResNet	0.585	0.630	0.631	0.800	0.799	0.819	0.803	0.738	0.809
ResNet-R	0.500	0.530	0.536	0.466	0.466	0.469	0.471	0.517	0.481
MobileNet	0.490	0.537	0.514	0.742	N/A	0.641	0.628	0.579	0.759
MobileNet-R	0.343	0.355	0.353	0.319	N/A	0.324	0.320	0.358	0.334
DenseNet	0.682	0.719	0.723	0.822	0.823	0.842	0.832	0.789	0.832
DenseNet-R	0.589	0.604	0.602	0.552	0.545	0.556	0.556	0.597	0.577
PGD-5	0.733	0.764	0.752	0.825	0.826	0.847	0.835	0.786	0.830
PGD-1	0.699	0.733	0.716	0.820	0.818	0.839	0.827	0.773	0.820

Table A9: Deletion for all 9 AM methods and 12 CNNs for experiment in Sec. 3.1 on **ImageNet-CL**. Bold numbers are the best CNNs for each AM method. As we stated in Sec. 3.5, we can observe that two CNNs with the lowest mean confidence are dominating Deletion; PGD-5 and DenseNet. The only case that none of them are winner is CAM in which we did not have MobileNet-v2 and AlexNet architecture.

	Gradient-based			CAM-based		Perturbation-based			
	Gradient	IG	SHAP	GradCAM	CAM	RISE	LIME	MP	EP
AlexNet	0.061	0.042	0.039	0.093	N/A	0.070	0.111	0.094	0.084
AlexNet-R	0.033	0.022	0.020	0.034	N/A	0.030	0.029	0.044	0.032
GoogLeNet	0.089	0.064	0.060	0.070	0.070	0.067	0.086	0.079	0.075
GoogLeNet-R	0.064	0.036	0.032	0.048	0.049	0.042	0.063	0.074	0.049
ResNet	0.125	0.086	0.077	0.115	0.115	0.108	0.108	0.125	0.122
ResNet-R	0.078	0.045	0.039	0.056	0.056	0.050	0.042	0.087	0.057
MobileNet	0.091	0.069	0.068	0.109	N/A	0.073	0.079	0.085	0.112
MobileNet-R	0.043	0.032	0.024	0.034	N/A	0.029	0.032	0.040	0.035
DenseNet	0.174	0.132	0.124	0.119	0.119	0.134	0.120	0.144	0.130
DenseNet-R	0.065	0.048	0.038	0.054	0.057	0.048	0.051	0.074	0.056
PGD-5	0.140	0.095	0.108	0.119	0.119	0.117	0.121	0.154	0.118
PGD-1	0.120	0.083	0.091	0.115	0.119	0.112	0.121	0.139	0.119

A6 Quantitative results of ImageNet

In this section, the quantitative results of experiment in Sec. 3.1 would be presented for our evaluation metrics for all CNNs and AM methods on ImageNet.

Table A10: Pointing game for all 9 AM methods and 12 CNNs for experiment in Sec. 3.1 on **ImageNet**. Bold numbers are the best CNNs for each AM method. In gradient-based methods, DenseNet-R is dominantly the best, and AdvProp’s CNNs in CAM-based methods outperform other CNNs.

	Gradient-based			CAM-based		Perturbation-based			
	Gradient	IG	SHAP	GradCAM	CAM	RISE	LIME	MP	EP
AlexNet	70.60	76.55	75.70	60.10	N/A	82.25	60.80	68.20	83.90
AlexNet-R	71.60	72.30	72.75	57.90	N/A	64.65	51.50	59.45	75.40
GoogleNet	74.25	79.55	78.90	86.35	86.35	87.35	71.85	70.90	89.40
GoogleNet-R	78.50	78.60	77.95	82.10	82.10	80.90	64.05	59.60	82.95
ResNet	64.75	70.90	73.45	86.15	86.20	89.60	73.45	71.50	88.10
ResNet-R	81.80	81.35	81.40	83.95	83.95	82.05	64.70	56.40	84.30
MobileNet	76.15	79.45	76.65	82.20	N/A	88.35	76.50	70.55	87.05
MobileNet-R	78.35	78.50	77.25	76.85	N/A	74.75	66.50	65.85	81.85
DenseNet	61.25	71.70	71.15	82.75	83.15	88.60	75.70	70.75	87.60
DenseNet-R	83.10	82.50	83.30	81.15	81.15	83.45	65.65	62.85	85.75
PGD-5	72.40	81.55	75.75	60.25	85.55	90.95	75.15	68.65	88.95
PGD-1	74.20	81.55	75.55	85.30	87.75	90.00	75.75	71.35	87.90

Table A11: WSL for all 9 AM methods and 12 CNNs for experiment in Sec. 3.1 on **ImageNet**. Bold numbers are the best CNNs for each AM method. As shown in Table A7, mostly robust CNNs are achieving the maximum score (6 out 9 AM methods).

	Gradient-based			CAM-based		Perturbation-based			
	Gradient	IG	SHAP	GradCAM	CAM	RISE	LIME	MP	EP
AlexNet	34.40	36.95	30.85	30.80	N/A	39.40	29.80	25.55	49.30
AlexNet-R	36.50	30.35	26.95	28.00	N/A	29.65	23.85	18.20	39.45
GoogleNet	40.90	41.15	38.80	56.75	56.35	43.20	39.35	31.25	49.35
GoogleNet-R	42.90	39.85	39.75	55.05	55.15	47.60	32.95	22.40	45.95
ResNet	35.55	36.20	35.65	56.55	56.85	45.55	38.45	29.30	47.05
ResNet-R	46.30	43.90	43.60	57.05	56.15	46.35	36.45	23.50	48.00
MobileNet	40.55	39.05	34.95	58.45	N/A	47.45	39.00	29.65	50.65
MobileNet-R	43.35	37.10	36.65	55.65	N/A	37.90	35.80	24.55	46.55
DenseNet	34.05	37.40	33.40	58.05	58.25	40.05	36.90	28.00	49.50
DenseNet-R	49.75	41.45	43.70	59.95	59.40	49.00	38.10	24.80	48.40
PGD-5	42.40	44.40	36.45	49.35	55.75	42.55	36.75	26.05	54.95
PGD-1	44.95	47.20	41.15	52.70	55.85	45.85	38.55	26.95	54.30

Table A12: Insertion for all 9 AM methods and 12 CNNs for experiment in Sec. 3.1 on ImageNet. Bold numbers are the best CNNs for each AM method. As shown, CNNs with high mean confidence tend to have higher higher Insertion.

	Gradient-based			CAM-based		Perturbation-based			
	Gradient	IG	SHAP	GradCAM	CAM	RISE	LIME	MP	EP
AlexNet	0.235	0.248	0.252	0.280	N/A	0.316	0.253	0.276	0.284
AlexNet-R	0.122	0.121	0.121	0.112	N/A	0.114	0.104	0.125	0.118
GoogleNet	0.300	0.319	0.324	0.384	0.384	0.422	0.378	0.367	0.390
GoogleNet-R	0.198	0.212	0.216	0.187	0.186	0.199	0.182	0.204	0.195
ResNet	0.397	0.425	0.426	0.559	0.559	0.587	0.564	0.517	0.564
ResNet-R	0.269	0.287	0.291	0.253	0.254	0.267	0.250	0.272	0.263
MobileNet	0.304	0.331	0.318	0.470	N/A	0.507	0.484	0.446	0.479
MobileNet-R	0.168	0.172	0.172	0.156	N/A	0.161	0.154	0.169	0.164
DenseNet	0.482	0.506	0.510	0.590	0.592	0.619	0.605	0.571	0.598
DenseNet-R	0.370	0.380	0.380	0.349	0.350	0.361	0.353	0.367	0.366
PGD-5	0.501	0.524	0.513	0.590	0.587	0.617	0.594	0.553	0.584
PGD-1	0.485	0.510	0.497	0.588	0.587	0.617	0.583	0.548	0.582

Table A13: Deletion for all 9 AM methods and 12 CNNs for experiment in Sec. 3.1 on ImageNet. Bold numbers are the best CNNs for each AM method. The same trend in Table A9 can be seen here that AlexNet-R is dominating the Deletion for all metrics except CAM that we did not have CAM for.

	Gradient-based			CAM-based		Perturbation-based			
	Gradient	IG	SHAP	GradCAM	CAM	RISE	LIME	MP	EP
AlexNet	0.027	0.020	0.019	0.036	N/A	0.029	0.047	0.039	0.037
AlexNet-R	0.014	0.009	0.008	0.014	N/A	0.010	0.010	0.017	0.014
GoogleNet	0.045	0.033	0.031	0.036	0.036	0.033	0.043	0.041	0.038
GoogleNet-R	0.031	0.017	0.015	0.024	0.023	0.020	0.030	0.031	0.024
ResNet	0.075	0.052	0.048	0.070	0.070	0.063	0.066	0.073	0.073
ResNet-R	0.044	0.026	0.022	0.031	0.032	0.026	0.040	0.043	0.033
MobileNet	0.052	0.039	0.038	0.063	N/A	0.054	0.060	0.068	0.066
MobileNet-R	0.023	0.017	0.013	0.018	N/A	0.015	0.015	0.021	0.019
DenseNet	0.114	0.086	0.082	0.078	0.078	0.089	0.077	0.091	0.085
DenseNet-R	0.042	0.031	0.024	0.035	0.035	0.031	0.033	0.044	0.038
PGD-5	0.081	0.057	0.063	0.071	0.072	0.068	0.075	0.086	0.070
PGD-1	0.070	0.049	0.054	0.068	0.072	0.065	0.074	0.082	0.072

Table A14: Correlation between four metrics on ImageNet. For ImageNet-CL correlation see Table 6b.

	Pointing game	WSL	Insertion	Deletion
Pointing game	1	0.81	0.38	0.15
WSL		1	0.30	0.15
Insertion			1	0.90
Deletion				1

A7 Heatmaps

This section is an extension for Fig. 1 to demonstrate the heatmaps of AM methods of different sample images from ImageNet-CL.

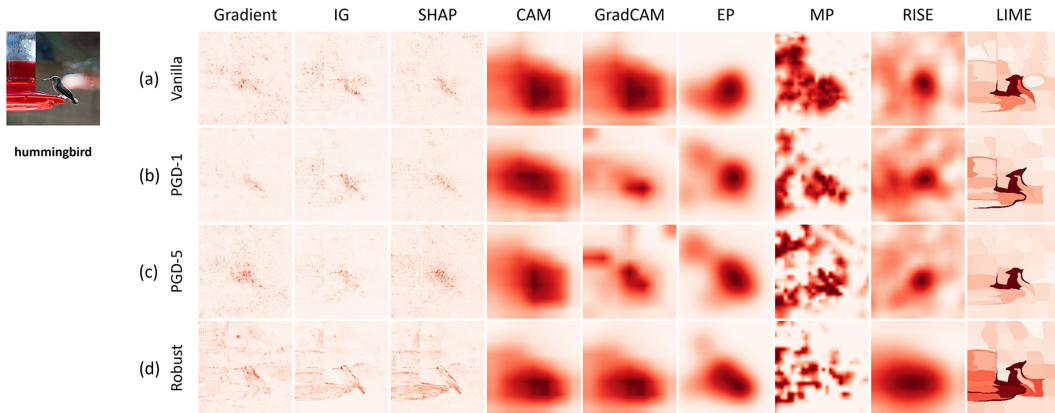


Figure A10: Heatmaps of 9 AM methods for four different CNNs of ResNet-50 architecture for the same input image of class “hummingbird”. From top down: (a) vanilla ImageNet-trained ResNet-50 [24]; (b–c) the same architecture but trained using AdvProp [56] where adversarial images are generated using PGD-1 and PGD-5 (i.e. 1 or 5 PGD attack steps [35] for generating each adversarial image); and (d) a robust model trained exclusively on adversarial data via the PGD framework [35]. We can see the same trend as we saw in Fig. 1 from top down, gradient-based methods’ AM are less noisy and more interpretable.

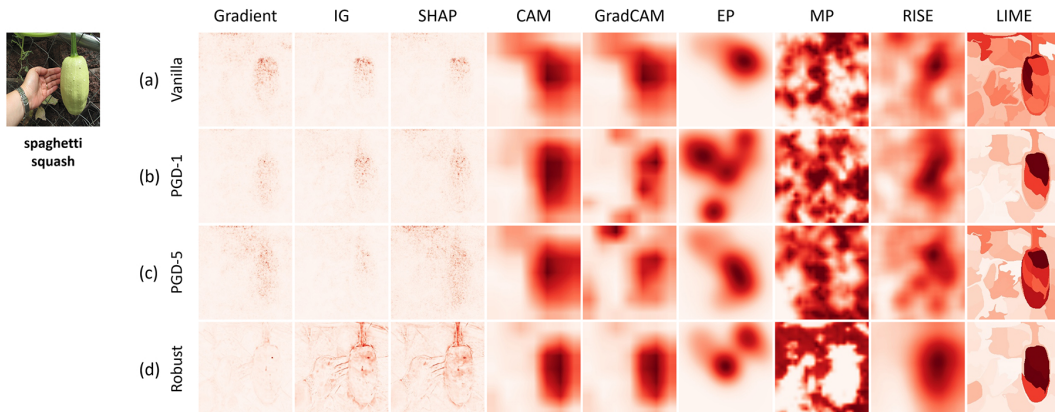


Figure A11: Heatmaps of 9 AM methods for four different CNNs of ResNet-50 architecture for the same input image of class “spaghetti squash”. From top down: (a) vanilla ImageNet-trained ResNet-50 [24]; (b–c) the same architecture but trained using AdvProp [56] where adversarial images are generated using PGD-1 and PGD-5 (i.e. 1 or 5 PGD attack steps [35] for generating each adversarial image); and (d) a robust model trained exclusively on adversarial data via the PGD framework [35]. We can see the same trend as we saw in Fig. 1 from top down, gradient-based methods’ AM are less noisy and more interpretable.

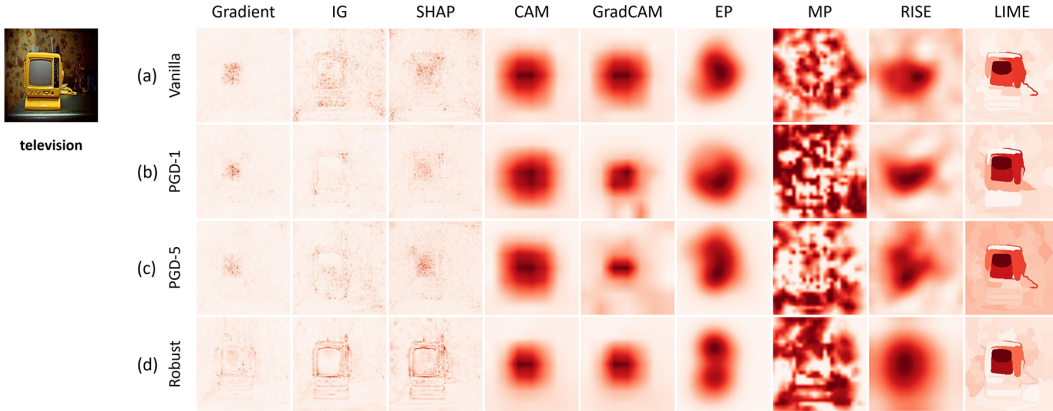


Figure A12: Heatmaps of 9 AM methods for four different CNNs of ResNet-50 architecture for the same input image of class “television”. From top down: (a) vanilla ImageNet-trained ResNet-50 [24]; (b–c) the same architecture but trained using AdvProp [56] where adversarial images are generated using PGD-1 and PGD-5 (i.e. 1 or 5 PGD attack steps [35] for generating each adversarial image); and (d) a robust model trained exclusively on adversarial data via the PGD framework [35]. We can see the same trend as we saw in Fig. 1 from top down, gradient-based methods’ AM are less noisy and more interpretable.

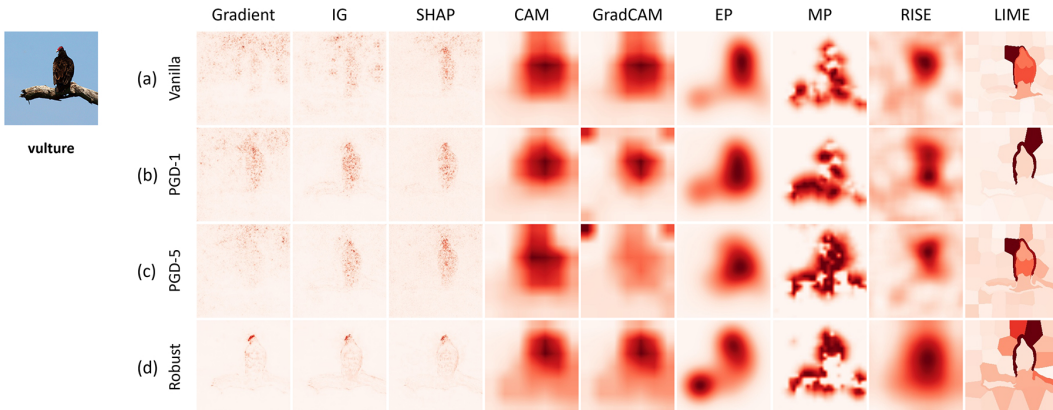


Figure A13: Heatmaps of 9 AM methods for four different CNNs of ResNet-50 architecture for the same input image of class “vulture”. From top down: (a) vanilla ImageNet-trained ResNet-50 [24]; (b–c) the same architecture but trained using AdvProp [56] where adversarial images are generated using PGD-1 and PGD-5 (i.e. 1 or 5 PGD attack steps [35] for generating each adversarial image); and (d) a robust model trained exclusively on adversarial data via the PGD framework [35]. We can see the same trend as we saw in Fig. 1 from top down, gradient-based methods’ AM are less noisy and more interpretable.